UNIVERSITY OF CALIFORNIA SAN DIEGO

Effects of the Phosphodiesterase 10A Inhibitor AMG 579 and *Pde10a2* Isoform Knockout on Striatal Regional Medium Spiny Neuron Marker and Immediate-Early Gene Expression in Rodents

A Thesis submitted in partial satisfaction of the requirements
for the degree Master of Science

in

Biology

by

Saumya Ranjan

Committee in charge:

Professor Christina Gremel, Chair
Professor Matthew Banghart, Co-Chair
Professor Monique Smith

2024

The Thesis of Saumya Ranjan is approved, and it is acceptable in quality and form for publication on microfilm and electronically.

University of California San Diego

2024

DEDICATION

For Mom and Dad and Kunal. With all my love.

TABLE OF CONTENTS

LIST OF FIGURES

LIST OF TABLES

LIST OF ABBREVIATIONS

cAMP	Cyclic adenosine monophosphate
cGMP	Cyclic guanosine monophosphate
CREB	cAMP-response element binding protein
DLS	Dorsal lateral striatum
DMS	Dorsal medial stratum
NAc	Nucleus accumbens
CPU	Caudate putamen
GPe	Globus pallidus externa
STN	Subthalamic nuclei
ERK	Extracellular signal-regulated kinase
CIE	Chronic Intermittent Ethanol
MSN	Medium Spiny Neuron
IEG	Immediate early gene
PDE	Phosphodiesterase
KO	Knockout
WT	Wild-type
AUD	Alcohol use disorder
qPCR	Quantitative polymerase chain reaction
RNA	Ribonucleic acid

ACKNOWLEDGEMENTS

Professional acknowledgments:

I would like to thank Dr. Amanda Roberts and the Scripps Research Animal Models Core Facility for the data collection for the mice CIE-exposure experiments (Supplemental Figure 2).

Personal acknowledgments:

I would like to thank everyone who I would like to thank for providing help and guidance throughout the process of my research and completing my thesis.

Firstly, I would like to thank my PI and mentor, Dr. Eric Zorrilla for his support and for giving me the opportunity to learn and grow in his lab over the past 2.5 years. His support, experience, and patience were invaluable over the course of my research and this thesis would not be possible without his help.

I would like to thank my committee members, Drs. Christina Gremel, Matthew Banghart, and Monique Smith, for their feedback and different perspectives which made me a better scientist and communicator. Thank you for all for taking the time to be part of my committee, I feel so honored to have you all be such an instrumental part of my defense.

I would also like to thank all the members of Zorrilla Lab who I've had the pleasure to interact with and learn from. I would like to give a special thank you to Drs. Luísa Bertotto and Cristiane Aparecida Favoretto, for answering my questions and helping me in my research journey. For setting such great examples for what a scientist looks like and for being such kind and supportive mentors. I would also like to thank Dr, Giovana Macedo for taking the time to get me started on my RNAscope experiment and for teaching me how to handle mice.

Lastly, I would like to thank my family and friends, who's unconditional love and support have gotten me through this experience. For my parents, I am deeply grateful for my

parents, for their love, care and encouragement. For the long phone calls, pep talks, and hugs when I needed the support. For the sacrifices they made to ensure a better life for me and my brother in the US. Your excitement and pride and wanting to be involved in my defense makes this accomplishment so much sweeter and satisfying. For Dhruv, for being there for me at the end of a long day, and for your calm and joyful demeanor for grounding me when I needed it most.

ABSTRACT OF THE THESIS

Effects of the Phosphodiesterase 10A Inhibitor AMG 579 and *Pde10a2* Isoform Knockout on Striatal Regional Medium Spiny Neuron Marker and Immediate-Early Gene Expression in Rodents

by

Saumya Ranjan

Master of Science in Biology

University of California San Diego, 2024

Professor Christina Gremel, Chair
Professor Matthew Banghart, Co-Chair

Alcohol use disorder (AUD) has major societal impact and few utilized treatments. New molecular targets with therapeutic potential and better understanding of the neurobiology of AUD are needed. Chronic ethanol exposure and consumption can lead to neurobiological changes in the brain's reward and motivation systems that are viewed as that perpetuate harmful drinking. The development of compulsive drinking putatively involves a shift in striatal control

from the NAc to the dorsomedial and then dorsolateral striatum as well as an imbalance between the dopamine receptor D1-direct and D2-indirect medium spiny neuron (MSN) pathways, whereby overactive dMSNs increase ethanol seeking and drinking behavior and underactive iMSNs putatively reduce inhibitory self-regulation. PDE10A is an enzyme of the phosphodiesterase enzyme family, a class of enzymes that regulate cellular responses by hydrolyzing cAMP/cGMP. PDE10A appears to encode the main PDE isoforms that control cAMP and cGMP levels of MSNs in the striatum, and the majority of PDE10A in the mouse striatum is the membrane-enriched PDE10A2 isoform. Recent studies suggest that inhibition of PDE10A family isoforms with different selective inhibitors can reduce alcohol self-administration in models of excessive or dependent intake, which has raised interest in PDE10A inhibitors as potential treatments for AUD. AMG 579 is a small molecule potent, selective PDE10A inhibitor that recently showed promise for its drug-like physiochemical properties (e.g., lipophilic efficiency) and ability to dose-dependently reduce ethanol consumption in rats. However, it is unknown how AMG 579 alters activation of striatal D1-direct and D2-indirect MSN pathways at doses that are considered effective to reduce drinking as well as whether there is regional variation or sex differences in these effects. There also is uncertainty as to the specific role of the PDE10A2 isoform in the anti-drinking or molecular actions of PDE10A inhibitors like AMG 579.

I decided to test the hypothesis that *Pde10a2*-knockout mice would show increased expression of *Drd1*, a direct pathway MSN marker, and the immediate-early genes (IEG) *Egr1* and *Fos* as compared to wild-type (WT) mice reflecting decreased regulation in cAMP due to *Pde10a2*-knockout (KO). I also hypothesized that treatment with the PDE10A inhibitor AMG 579 would increase IEG expression, similar to what was observed previously with the PDE10A

inhibitors MR1916 and TAK-063. Further, I hypothesized that treatment effects seen on IEG expression would be in wild-type mice only, which would indicate that the membrane-bound PDE10A2 isoform was involved in the ability of the PDE10A inhibitor to alter MSN activation, and thus absent in *Pde10a2*-knockout mice. These results were expected to be more pronounced in the dorsal striatum than the NAc, because PDE10A mRNA and protein are expressed at greatest levels in the caudate-putamen, and in male animals more their female counterparts, due to previously reported sex differences in synaptic striatal PDE10A levels and activation effects of the PDE10A inhibitor papaverine in vitro.

MSN marker expression was measured using two methods: qPCR to measure overall *Drd1*, *Drd2*, *Penk*, *Fos*, and *Egr1* expression and a method of fluorescent *in-situ* hybridization known as RNAscope to measure *Drd1*, *Drd2* and *Egr1* expression within *Drd1*- and *Drd2*-positive cell types. qPCR results show that both treatment with AMG 579 and *Pde10a2*-knockout decreased expression of *Drd1*, *Drd2*, *Fos*, and *Egr1*. *Pde10a2*-knockout seemed to reduce *Penk* expression as well. There were trends that suggested that there was a stronger reduction in *Drd2* expression in AMG 579 KO mice in males than females but not in expression in *Pde10a*, *Drd1*, or either of the IEGs.

RNAscope results showed that *Egr1* expression within *Drd1*- and *Drd2*-expressing cells types as well as undefined cell types decreased as a result of treatment with AMG 579. The DMS and, to a lesser extent, the DLS, showed greater significance in Treatment effect than the NAc. Treatment with AMG 579 seemed to have a sexually dimorphic effect in the DMS that varied by gene target or cell type. Overall, the results show that AMG 579 acts differently than other PDE10A inhibitors in that it reduces, instead of increases, MSN marker and IEG expression;

further study is needed to determine which method is better suited to modulate problematic drinking behavior.

Chapter 1: Introduction

Alcohol use disorder (AUD) affects millions of Americans every year, and its increasing prevalence over the last decade [1] has a massive community impact. Indeed, AUD is one of the most common psychiatric disorders in the United States [2], and even though it increases morbidity 6-fold [3], pharmacotherapy for alcohol use is significantly underused [4]. Less than 1 in 5 individuals who had AUD in their lifetime ever received treatment [1], and one quarter of those in remission relapse within 3 years [5]. With excessive alcohol drinking and its related comorbidities, such as heart disease, cancer, and conditions of the liver, gallbladder, and pancreas [6], costing the US over $200 billion per year [7], there is a need for suitable drug targets to treat AUD and better understanding of how AUD works on the neurobiological level.

Chronic ethanol exposure and consumption can lead to neurobiological changes in the brain's reward and motivation systems that are viewed as maladaptive and perpetuating harmful drinking For example, it has been hypothesized that chronic alcohol intake modifies dopamine D1 receptor positive (D1)-direct and dopamine D2 receptor positive (D2)-indirect pathway medium spiny neuron (MSN) pathway in the striatum. In the striatum, there are two heuristically and neurochemically distinct MSN pathways, each expressing different molecular markers. Direct pathway MSNs (dMSNs) project directly to basal ganglia output regions and express the genes that encode dopamine D1 receptors (*Drd1*), substance P (*Tac1*), and prodynorphin (*Pdyn*) as molecular markers. Indirect pathway MSNs (iMSNs) indirectly reach basal ganglia output by projecting to the globus pallidus externa (GPe) and subthalamic nuclei (STN) and express dopamine D2 receptors (*Drd2*), adenosine 2A receptors *(A2a),* and proenkephalin (*Penk*).

The balance between D1-direct vs. D2-indirect MSN activation has been viewed as instrumental in subserving motivated and motor behavior [8]. Heuristically, the activation of the

D1-direct pathway is associated with goal-seeking behavior ("Go" behavior) and appetitive, approach responses; in contrast, activation of the D2-indirect pathway is associated with stop ("NoGo" behavior) or avoidance behavior and aversive responses [9]. On a molecular level, activation of D1-receptors leads to an increase in cell signaling and synthesis of cAMP while conversely, activation of D2-receptors inhibits cell signaling and the production of cAMP [10,11]. During chronic ethanol consumption, both D1 and D2 pathways have been hypothesized to be modified in a way that contributes to problematic ethanol intake. D1-MSN activation is increased, resulting in increased ethanol drinking behavior, while the D2-MSN activation is reduced, resulting in fewer "NoGo" responses, manifesting as decreased self-regulation in ethanol consumption [12]. Because relatively underactive iMSNs or overactive dMSNs have been proposed to lead to compulsive ethanol consumption [13–16] a focus on repairing this balance on the molecular level is a proposed strategy for developing new treatments for AUD.

PDEs are a class of enzymes that regulate diverse cellular responses by breaking down and thereby functionally inactivating cyclic adenosine 3′, 5′-monophosphate (cAMP) and/or cyclic guanosine 3′, 5′-monophosphate (cGMP) [17,18]. PDEs are encoded by 21 genes that produce more than 50 different enzymes [19]. Supporting a role for PDEs in the regulation of ethanol intake, the pan-PDE inhibitor ibudilast has been shown to decrease ethanol drinking in alcohol-preferring rats, high-alcohol drinking rats, ethanol-dependent mice, and in early clinical studies, people [20,21]. However, the role of particular PDE families remains unclear. The functional role of any particular PDE-family enzyme is defined by where it is expressed in the body. For example, PDE5 plays a role in regulating vascular vessels and in the central nervous system, and is found in highest concentrations in the cerebellum, kidney, and pancreas [22,23]. In contrast, PDE10A is a PDE that is differentially expressed in striatal MSNs, and is the main

PDE isoform that controls MSN cAMP and cGMP levels [24,25]. The PDE10A sub-isoform, PDE10A2, is found in highest concentrations in the striatum, making it an ideal candidate for modulating signaling in the D1-direct and D2-indirect pathways [19,26]. PDE10A2 is not the only PDE10A sub-isoform, as PDE10A19 is a primate-specific PDE10A isoform that is also expressed in the striatum and is thought to interact with and direct the position of PDE10A2, from membrane-bound position to a cytosolic one and is thought to play a role in the development of bipolar disorder [27].

Previous studies using family-selective PDE inhibitors have linked the activity of PDE4 and PDE10A in particular, with regulation of ethanol intake [28–30]. With regard to PDE10, previous studies have also revealed that alcohol use increases availability of the striatal enzyme phosphodiesterase 10A (PDE10A), supporting a possible role in alcohol intake [31]. Furthermore, systemic administration of the PDE10A inhibitor MP-10 has been seen to activate *Drd2*-expressing medium spiny neurons (MSNs) to a greater extent than *Drd1*-expressing MSNs [32], suggesting that while they can influence both D1 and D2 pathways, some PDE10A inhibitors may shift balance to greater relative iMSN activation.

There is also evidence that TP-10, a tool-like PDE10A inhibitor, decreased alcohol self-administration in rats [29], which makes PDE10A a promising molecular target for AUD. Recent work in the lab with MR1916 [33] and, more recently, AMG 579 [34] further support that PDE10A inhibitors can reduce ethanol self-administration. The aim of this study is to further test the hypothesis that striatal PDE10A, implicated in the modulation and effects of ethanol intake, may modulate activity of direct vs. indirect pathway MSNs. For this, I study the effects of AMG 579, a small molecule selective PDE10A inhibitor, and genetic knockout of the PDE10A2 isoform.

Chapter 2: Immediate-Early Gene and MSN Marker mRNA Expression After AMG 579

As reviewed, PDE10A is an emerging molecular target for AUD treatment, but how a dose of PDE10A inhibitor that influences ethanol intake modulates D1-direct and D2-indirect MSN activity is unknown. One can infer a role for PDE10A in modulating specific brain pathways by measuring changes in pathway activity that occur when the enzyme is inhibited via selective inhibitors. One way to determine such effects is to measure the effect of PDE10A inhibitors on expression of immediate-early genes (IEGs), rapid primary response genes used as indices of recent neuronal activation [35]. Given PDE10A's molecular action to hydrolyze cAMP and cGMP, the expression of IEGs whose transcription is responsive to cAMP/cGMP signaling, like *Fos* and *Egr1*, are readouts of special interest [36–41]. Measuring the change in IEG expression can help to quantify the effects of PDE10A inhibitors. Alternatively, the effect a PDE10A inhibitor has can be determined by comparing its effects on expression of dMSN vs. iMSN markers (like *Drd1* and *Drd2*, respectively) that may serve as potential indices of actions on direct or indirect-pathway cell subpopulations. PDE10A inhibitors can augment activation of both dMSNs and iMSNs [33,42,43], but not necessarily to equal degrees. Some inhibitors enhance dMSN expression while others can be iMSN biased. These differences in MSN marker effects have been hypothesized to be due to differences in enzyme off-rate, with fast off-rate PDE10A inhibitors being iMSN-biased while slow-off rate ligands instead showing balanced or dMSN-biased activation [44]. The different actions are hypothesized to reflect greater basal cAMP/cGMP activity, and thereby requirements for more sustained PDE10A inactivation, within D1-dMSNs vs. D2-iMSNs [44].

Previous studies of PDE10A inhibitors have shown promising results to reduce intake in models of high ethanol intake. An early set of studies found that TP-10 reduced alcohol self-

administration in male rats during acute ethanol withdrawal, following a history of stress, or in a genetically-selected model of alcohol preference [30]. However, this study did not look at the effects of PDE10A inhibition in female rats, and sex differences are possible based on findings that there are sex differences in synaptic levels of PDE10A [45] and in the in vitro effects of the PDE10A inhibitor papaverine on ERK1/2 phosphorylation [46]. Indeed, the PDE10A inhibitor MR1916 recently was found to show sex differences in its ability to reduce ethanol self-administration and induce immediate-early gene expression in the striatum of male vs. female rats [33].

On the other hand, the clinical candidate AMG 579, a PDE10A inhibitor that shows high promise for possessing physiochemical properties (e.g., lipophilic efficiency [LipE]>5 [47–50]) that are more drug-like than other studied PDE10A inhibitors, like TP-10, MP-10, MR1916, and papaverine, was observed to potently reduce ethanol self-administration in post-dependent rats of both sexes [51] (see Supplemental Figure 1). Still unknown is how AMG 579 alters MSN activation at doses that reduce ethanol self-administration and whether there are sex differences in these effects [46,52]. Most previous studies that have investigated the impact of PDE10A inhibitors on dMSN and iMSN pathway activation have studied doses that are cataleptic and substantially higher than those that specifically reduce drinking [29,53]. Therefore, the effects of the lower doses that reduce ethanol drinking on MSN activation remain poorly understood.

I therefore wanted to see if injection with AMG 579 would also affect activation of immediate early genes (IEG) as a sign of neuronal activation and whether these effects differ between D1-MSN vs. D2-iMSN or by sexes. Initial findings from this lab suggest that in mice, AMG 579 significantly reduces voluntary ethanol consumption in post-dependent, CIE-exposed mice. To understand the effects of this dose on MSN activation, I therefore studied a promising

dose (100 nmol/kg dose, i.p.) from this study in the range that was also found to not non-specifically alter locomotor behavior in photocell cage [34]. Based on these results, this dose was used to study the effect AMG 579 has on MSN marker and IEG expression in mice using qPCR.

The PDE10A2 isoform contains a unique amino-acid trafficking sequence that allows it to be localized to the dendritic membrane to regulate MSN responses to afferent (e.g., cortical) input [22,54,55]. This key regulatory role is seen in the increased levels of cAMP and phosphorylated CREB in the striatum of *Pde10a2*-knockout (KO) mice [26]. Thus, I hypothesize that the *Pde10a2* KO mice will have an increase in *Drd1* expression compared to the wild-type mice as a result of this decrease in cAMP/cGMP cascade inactivation. I hypothesize to see a similar direction of Treatment effect of acute AMG 579 administration on IEG expression, but only in wild-type mice only, which would indicate that inhibition of the membrane-bound *Pde10a2* isoform is responsible for the MSN-activating effects of PDE10A inhibitor and is thus absent in *Pde10a2* KO mice. I predict that the AMG 579 treatment will increase both *Drd1* and *Drd2* expression, similar to other PDE10A inhibitors like MR1916 and TAK-063 [33,44]. Like other PDE10A inhibitors, like MP-10 [42], I predict that treatment with AMG 579 will increase IEG expression, with a greater effect on *Egr1* vs. *Fos*. Finally, I predict that inhibitor and genotype effects will be more pronounced in male mice, because the PDE10A inhibitor papaverine less effectively altered ERK1/2 activation in striatal tissue of female mice compared to male and ovariectomized female rats [46].

Chapter 2.1: Methods

Subjects:

Adult (~7 months old) male and female C57BL/6J mice were studied for striatal gene expression (n=41-43/ sex). Mice were maintained in a temperature- (20-23°C) and humidity-controlled (30-70%) vivarium under a reverse dark light cycle (lights on 9pm, off 9am). Mice had *ad libitum* access to food (Product Number: 2018, Teklad Diets) and tap water. *Pde10a2*-deficient ("KO") mice were created using homozygous knock-in/knockout of a disrupting tetracycline transactivator (tTA) construct after the start codon for the *Pde10a2* specific exon [26]. Founders of the KO mouse line (*Pde10a2*$^{tm1(tTA)Yok}$) were provided generously by Dr. Hiromi Sano, and subjects were homozygote *Pde10a2* mutant allele (knockout) offspring of heterozygote/heterozygote breeding or their respective homozygote *Pde10a2* wildtype littermates from an in-house breeding colony. All mice were genotyped at weaning before study inclusion from tail DNA. All procedures conformed to the National Institutes for Health *Guide for the Care and Use of Animals* and were approved by the Institutional Animal Care and Use Committee of Scripps Research Institute.

Experimental Design and Tissue Collection

To determine the effects of the PDE10A inhibitor AMG 579 and *Pde10a2* isoform KO, the study involved a 2 (Genotype: *Pde10a2* KO or WT) x 2 (Treatment: vehicle or 100 nmol/kg AMG 579) x 2 (Sex: Male or Female) between-subject factorial design. The first phase was the sample collection step. Striatal brain punches were collected from 84 PDE10A2$^{tTA/tTA}$ (n=26 male, 23 female) and 35 wild-type mice (n=17 male, 18 female) that were around 7 months old (*M* ± SEM of age: male KO: 211.35 ± 4.75 days old, male WT: 201.59 ± 2.52 days old, female KO: 214.63 ± 4.01 days old, female WT: 202.72 ± 2.63 days old). After letting them acclimate to

the reversed dark light cycle and regular handling and weighing for 2 weeks, mice were then intraperitoneally injected with the drug candidate AMG 579 (100 nmol/kg) or 10% *w/v* 2-Hydroxypropyl-β-cyclodextrin (HPBC) (Sigma Catalog Number: 778907) vehicle dissolved in Nanopure water (10 ml/kg). Specific sample sizes by sex were, for males: 9 WT -vehicle, 8 WT-AMG 579; 12 KO-vehicle, 14 KO-AMG 579; and, for females: 9 WT-vehicle, 9 WT-AMG 579; 7 KO-vehicle, 16 KO-AMG 579. Mice were then placed back into their home cage with access to food and water. The mice were then sacrificed 90 minutes post-injection by decapitation after being rapidly anaesthetized (~1 min) with isoflurane. Brains were dissected on an ice-cold stage, coronally-sectioned (~1-1.5 mm slices), and punches were then taken of the DLS and NAc from both hemispheres using a blunt 13-gauge spinal needle. The tissue was placed in a 1.5 ml centrifuge tube, flash-frozen in liquid nitrogen, kept on dry ice post-dissection, and then stored in a -80 °C freezer until subsequent RNA processing.

RNA extraction, reverse transcription, and qPCR

For RNA analysis, total RNA was then extracted from each of the samples using QIAzol lysis reagent (Qiagen Catalog Number: 79306) with cellular disruption using a discardable pestle and pestle motor, followed by cleaning with the Zymo Research Clean and Concentrator-25 (Zymo Catalog Number: R1018). RNA quality and concentration were measured with Nanodrop 2000c (Thermo Fisher Catalog Number: ND-2000C) (M ± SEM of RNA concentration: 290.5±7.9 ng/µl; A260/280: 2.0±0.003, A260/230: 1.9±0.02). Low quality samples (defined as concentration <10 ng/µl, A260/280 < 1.8, or A260/230 <1; n= 6/163, 3.6% of total samples collected) were excluded.

Samples (~300ng total RNA input /sample) were ezDNase-treated and then reverse-transcribed using SuperScript IV (SSIV) reverse transcriptase (RT) VILO kit (Thermo Fisher Catalog Number:11766050) following the manufacturer's instructions to form cDNA to be used in a quantitative polymerase chain reaction (qPCR). cDNA was diluted with nuclease-free water (final concentration: 1 ng/µl) to yield aliquots, stored at -80 °C until performing qPCR. Gene expression levels were measured with qPCR, using Applied Biosystems PowerTrack SYBR Green (Thermo Fisher Catalog number A46110) in a QuantStudio5 Real-Time PCR instrument (Thermo Fisher Catalog number: A28135) in a 384-well system on the following genes targets: *Pde10a2*, *Drd1*, *Drd2*, *Penk*, *Egr1*, *Fos*. *18s* was used as the reference housekeeping gene. Primer pairs, shown in Table 1, were obtained from Integrated DNA Technologies. To reduce assay-to-assay variation, all samples for a given primer pair were run within a single plate and reaction run. The qPCR conditions for all primer pairs were: 95°C denaturation temperature for 15 seconds; 60.3°C annealing temperature for 15 seconds, and 72°C extension temperature for 15 seconds. Samples were analyzed in duplicate, with nuclease-free water used as a negative control. Gene-specific amplification was determined by melt curve analysis as one peak at the expected PCR product melting temperature.

Table 1: Forward and reverse primer sequences used for qPCR

Gene Name	Forward Primer	Reverse Primer
Pde10a2	5'-TTG CCA CCG TTT GGC CG	5'-GCT GAG GAA ACA CTC GGT CA
Egr1	5'-TCG GCT CCT TTC CTC ACT CA	5'-CTC ATA GGG TTG GCT CGG
Fos	5'-CAG CCT TTC CTA CTA CCA TTC C	5'-ACA GAT CTG CGC AAA AGT CC
Drd1	5'-GAC ATA CGC CAT TTC ATC CTC C	5'-ATG CGC CGG ATT TGC TTC T
Drd2	5'-CCT TAA GAC GAT GAG CCG CAG GA	5'GGT TCA CGG CAC TGT TGA CAT AGC
Penk	5'-TTC AGC TCG GCG GCG TTG	5'-GAA GCG AAC GGA GGA GAG AT
18s	5'- GCA ATT ATT CCC CAT GAA CG	5'-GGC CTC ACT AAA CCA TCC AA

Data Analysis

Quality control was first applied to qPCR results. Specifically, samples with low-quality Ct scores for *18s* (defined as Ct >18 cycles, 8/157, 5.1% of total samples), incorrect genotype labelling (nominally KO mice exhibiting *Pde10a2* expression Ct <20 cycles or nominally WT mice with *Pde10a2* expression Ct >35 cycles, 2/157, 1.3% of total samples), or multiple outlier values (defined by 3+ gene targets with outlying Ct values per Dixon's Q-test, 1/157, 0.64% of total samples) were excluded. Additionally, potential outliers were defined a) using the Dixon's Q-test [56,57] (on raw Ct data) and b) as z-scored values that had high studentized residual scores (≥|3.0|) combined with either undue leverage (>2-fold the jackknifed mean leverage of other samples) or influence (Cook's D >the 50%ile of the F-distribution, F[Cook's D](k+1,n-k-1), where k=number of predictor variables and n=total samples) [58]. Identified outliers (2/876, 0.23% of qPCR values) were replaced using multiple imputation [59] as the average of 10 independent estimates in SPSS. The z-scores of the ΔΔCT scores for each target gene within each region were calculated to compare expression between target genes. The *18s* housekeeping

gene was used as the reference gene when calculating the ΔCt for each target gene. I used the vehicle-WT males as the reference group for each region when calculating the ΔΔCT scores. The z-scores of ΔΔCt scores (multiplied by -1 for directionality) for each region were analyzed using a 3-way univariate GLM in SPSS with Genotype, Sex, and Treatment as factors. Each region (DLS and NAc) was normalized separately within itself and was not considered a statistical factor due to significant differences in *18s* expression between the DLS vs. NAc. Statistically significant effects were defined as $p<0.05$.

Chapter 2.2: Results

MSN marker expression

Pde10a2

As Figure 1A shows, in the DLS, as expected, there was a significant Genotype effect with the *Pde10a2* KOs expressing significantly less *Pde10a2* compared to the WT mice [$F(1,65)=502.888$, $p<0.001$]. There were no significant main or interaction effects involving Treatment or Sex on DLS *Pde10a2* expression.

As Figure 1B shows, in the NAc, as expected, there was a similar large Genotype effect like what was seen in the DLS [$F(1,65)=554.766$, $p<0.001$]. There was also a significant Treatment effect, with AMG 579 reducing *Pde10a2* expression [$F(1,65)=4.440$, $p=0.039$]. There were no significant main or interaction effects involving Sex on NAc *Pde10a2* expression.

Drd1

As Figure 2A shows, in the DLS, there was a Genotype main effect whereby *Pde10a2* KO mutants had less *Drd1* expression than the WT controls [$F(1,65)=7.662$, $p=0.007$]. A Treatment effect reflected that AMG 579 also reduced *Drd1* expression [$F(1,65)=4.755$, $p=0.03$]. Interestingly, there was a trend for a 2-way Treatment X Genotype interaction [$F=(1,65)=3.275$, $p=0.075$]. Pairwise follow-up comparisons to interpret the interaction showed that, AMG 579 significantly reduced *Drd1* expression in the KO mice [$F(1,65)=9.343$, $p=0.003$] as compared to the KO mice that received vehicle. However, there was no significant Treatment effect seen in the wild-type mice [$F(1,65)=0.060$, $p=0.807$]. Consequently, drug-treated KO mice showed reduced *Drd1* expression compared to WT mice given drug [$F(1,65)=11.570$, $p=0.001$] a Genotype difference not seen in vehicle-treated mice. There were no main or interaction effects involving Sex in DLS *Drd1* expression.

As Figure 2B shows, in the NAc, there was a significant Genotype main effect [$F(1,65)=5.375$, $p=0.004$], again reflecting reduced *Drd1* expression in the *Pde10a2* KO mice, compared to the WT group. There was also a significant Treatment main effect [$F(1,65)=9.096$, $p=0.004$] in which AMG 579 again decreased *Drd1* expression in the NAc. Unlike what was seen in the DLS, this Treatment effect was seen in both KO and WT mice, demonstrating that the inhibitor decreased *Drd1* expression independent of *Pde10a2* knockout.

Drd2

As shown in Figure 2C, in the DLS, there was a significant Genotype effect whereby the KO mice had a significant decrease in *Drd2* expression compared to the WT [$F(1,65)=7.844$, $p=0.007$]. A trend for a Treatment main effect reflected that AMG 579 tended to reduce *Drd2* expression overall [$F(1,65)=3.643$, $p=0.061$]. Additionally, a trend for a 3-way Treatment X Genotype X Sex interaction was observed [$F(1,65)=3.376$, $p=0.071$] which reflected that AMG 579 treatment differentially reduced *Drd2* expression in male knockout *Pde10a2* KO mice. Pairwise comparisons to interpret the trend showed that AMG 579 significantly decreased *Drd2* expression only in KO males vs. their vehicle controls [$F(1,65)=13.175$, $p<0.001$]. Consequently, KO males that received AMG 579 had less *Drd2* expression than KO females [$F(1,65)=8.771$, $p=0.004$] and also WT males [$F(1,65)=13.480$, $p<0.001$] with the same treatment. Other than the interaction already listed, there were no differences amongst AMG-treated wildtype groups.

As Figure 2D shows, in the NAc, there was a significant Treatment effect, in which AMG 579 again significantly decreased *Drd2* expression [$F(1,65)=5.436$, $p=0.023$] independent of

Genotype and Sex. There was a trend for Genotype-dependent reduction of *Drd2* in the knockout mice [$F(1,65)=3.334$, $p=0.072$], but no main or interaction effects involving Sex.

Penk

As seen in Figure 2E, in the DLS, there was a significant reduction in *Penk* expression due to Genotype in the KO mice [$F(1,65)=25.523$, $p<0.001$]. There were no main or interaction effects involving Treatment or Sex.

As Figure 2F shows, in the NAc there was a similar Genotype main effect, reflecting that *Pde10a2*-KO mice had reduced *Penk* expression [$F(1,65)=21.990$, $p<0.001$).There also were trends for a Treatment-effect of AMG 579 to reduce *Penk* expression in the NAc [$F(1,65)=3.565$, $p=0.063$], and a 3-way Treatment X Genotype X Sex interaction [$F(1,65)=3.594$, $p=0.062$]. Pairwise comparisons to interpret the interaction trend showed that were significant Genotype-dependent decreases in *Penk* expression whereby KO female mice that received AMG 579 [$F(1,65)=6.608$, $p=0.012$], or vehicle [$F(1,65)=11.938$, $p<0.001$] had reduced Penk expression vs. their respective WT controls, a similar finding as seen for KO male mice that were treated with AMG 579 [$F(1,65)=7.313$, $p=0.009$].

IEG expression

Egr1

As shown in Figure 3A, in the DLS, there was a significant Treatment main effect that unexpectedly reflected a decreased *Egr1* expression in mice treated with AMG 579 [$F(1,65)=14.229$, $p<0.001$]. There was a trend for a Genotype main effect, whereby the *Pde10a2*

KO mice also had a decrease *Egr1* expression than their WT controls. [$F(1,65)=3.40$, $p=0.069$], but no main or interaction effects involving Sex.

As seen in Figure 3B, in the NAc a similar Treatment main effect was seen as in the DLS, whereby AMG 579 decreased *Egr1* expression [$F(1,65)=5.587$, $p=0.021$]. There were no main or interaction effects involving Sex or Genotype.

Fos

In both the DLS (Figure 3C, $F(1,65)=8.730$, $p=0.004$) and NAc (Figure 3D, $F(1,65)=12.863$, $p<0.001$), there was a Treatment main effect whereby AMG 579 unexpectedly reduced *Fos* expression. In both regions, there were no main effects or interactions involving Genotype or Sex.

Genotype-specific analysis

For both IEGs, there was a significant main effect of treatment. However, descriptively, the male KO mice did not appear to show a Treatment effect and when analyzing the AMG 579 treatment effects separated by genotype, there only was a significant Treatment main effect of AMG 579 in WT mice [DLS, *Fos*: $F(1,26)=4.319$, $p=0.048$; *Egr1*: $F(1,26)=6.247$, $p=0.019$; NAc, *Fos*: $F(1,25)=8.496$, $p=0.007$); *Egr1*: $F(1,25)=6.255$, $p=0.019$] and not for KO mice [DLS, *Fos*: $F(1,39)=3.769$, $p=0.059$; NAc, *Fos*: $F(1,40)=3.397$, $p=0.073$); *Egr1*: $F(1,40)=0.879$, $p=0.354$] Still, however, a significant interaction involving Treatment X Genotype was not observed in the initial 3-way model.

Chapter 2.3: Discussion

The observed outcome of the PDE10A inhibitor AMG 579 diverged from what was hypothesized. Unlike other PDE10A inhibitors that reportedly increased MSN marker and IEG expression [33,42,44], AMG 579 did the opposite and decreased expression of all IEGs and MSN markers. The reductions in MSN marker expression did not appear to be *Pde10a2*-dependent in the NAc, because the magnitude of reduced *Drd1*, *Drd2*, and *Penk* marker expression was similar in PDE10A2$^{tTA/tTA}$ KO vs. wild-type mice. Quite unexpectedly, AMG 579, if anything, appeared to differentially reduce *Drd1* and *Drd2* expression in *Pde10a2* KO and not wildtype mice, implicating compensatory or downstream changes in other PDE10A isoforms. Conversely, AMG 579 elicited significant reductions of *Egr1* and *Fos* marker expression in WT mice that were descriptively larger than in KO mice, in which significant changes were not observed separately. This effect was seen in both regions and sexes, and unexpectedly, independent of genotype. Altogether, the results indicate that the ability of AMG 579 to reduce MSN marker expression is not dependent on the *Pde10a2* isoform being present, while its ability to reduce IEG expression might be.

Changes in MSN marker expression in AMG 579-treated mice

AMG 579 was hypothesized to increase both indirect pathway activation and direct pathway activation, as has been reported for other PDE10A inhibitors [33,44]. MSN marker expression has been used as an index of pathway activation after PDE10A manipulation [44,60]. Unlike MR1916 and TAK-063, AMG 579 decreased expression of the potential indirect pathway marker *Drd2* in both striatal subregions, with a significant decrease in the NAc and as a trend in the DLS. AMG 579 also significantly decreased expression of the direct pathway marker *Drd1* in

both regions and genotypes as well. Because AMG 579 reduced MSN marker expression within the NAc similarly between WT and *Pde10a2*-KO mice, the results suggest that the actions of the PDE10A inhibitor to reduce *Drd1* and *Drd2* expression did not require the PDE10A2 isoform. Possible explanations for this findings is that these effects of AMG 579 were mediated by one of the other PDE10A, non-membrane-associated, isoforms known to be expressed in striatum [53,61] or, alternatively, that AMG 579 has unrecognized "off-target" pharmacological effects other than PDE10A inhibition. Studies with a pan-PDE10A KO or knockdown model could be used to test the latter hypothesis, but these mice do not currently exist, because formerly created pan-PDE10A mutants were eliminated by Pfizer and Merck (Sean Smith, personal communication to Dr. Zorrilla).

Within the NAc, where AMG 579 significantly reduced the expression of *Drd1* and *Drd2*, the reduction in *Drd2* was similar to or only marginally greater than that for *Drd1* expression (mean difference in z-scores: -0.905 vs. -0.795, respectively). This comparison relates to the hypothesis that different PDE10A inhibitors might have different influences on the activity and balance between D1 vs. D2 pathways based on differences in their molecular properties. For example, compounds with a faster off-rate such as TAK-063 have been interpreted as showing iMSN-biased activation, whereas slow-off rate ligands such as MP-10 instead show balanced or dMSN-biased activation [44]. Here instead, there was apparent observed inhibition of both pathways, as indicated by *Drd1* and *Drd2* markers, following AMG 579, with only marginally greater reduction of the iMSN marker.

The AMG 579-induced reduction in *Drd1* and *Drd2* MSN marker expression was unexpected given previous reports that MR1916, MP-10, and TAK-063 all increased expression of *Drd1* or *Drd2* MSN markers [33,60,62]. Similarly, treatment with AMG 579 reduced

expression of the pan-marker, *Pde10a2*, in the NAc, and in the iMSN subpopulation marker, *Penk*, in the male KO population, suggesting that the compound generally decreased MSN marker expression.

Changes in Direct Pathway MSN Marker Expression due to Genotype-Effects

I hypothesized that *Pde10a2* KO mice would show increased *Drd1* expression because the associated decrease in cAMP hydrolysis would lead to greater MSN activation. Indeed, previously, this mouse KO line has been reported to show increased striatal cAMP and CREB phosphorylation [26]. Instead, however, here decreased striatal *Drd1* expression was seen in both regions, with KO mice having a lower mean z-score than WT (mean difference in z-scores in DLS: -0.798; NAc: -0.611), with a similar change in *Drd2* (mean difference in z-scores in DLS: -0.816; NAc: -0.709) and *Penk* (mean difference in z-scores in DLS: -1.955; NAc: -1.390) expression in *Pde10a2* KO vs. WT mice. This unexpected direction of result corresponds with the direction of effect (reduced *Drd1* expression) seen after treatment with the PDE10A inhibitor AMG 579, though that pharmacological effect does not appear to be *Pde10a2*-dependent. Nonetheless, the results support the hypothesis that *Pde10a2* may play a key role in regulating *Drd1* expression or pathway activity.

It cannot be ruled out that the unexpected direction of effect reflects a potential role of compensatory changes in other PDE10A isoforms, such as PDE10A1, which has been observed to be upregulated by 55% in PDE10A2$^{tTA/tTA}$ KO mice in comparison to the striatum of wild-type mice [26], or even in other striatal PDEs, such as PDE4 [63], since they were not measured in the present study. Measurement or joint inhibition of potential compensatory isoforms could help test these alternative explanations.

Genotype-Related Changes in AMG 579 Effects on MSN Expression in the DLS

I hypothesized that AMG 579 would alter IEG and MSN expression in the wild-type mice only, which would indicate that the membrane-bound PDE10A2 isoform was required for and potentially mediated activating effects of the PDE10A inhibitor. Instead, the results showed that for DLS *Drd1* and *Drd2* expression, AMG 579, quite the opposite, differentially reduced *Drd1* and *Drd2* expression in KO and not in WT mice. The results suggest that loss of *Pde10a2* increased functional significance of another *Pde10a* isoform or other molecule in the DLS with which AMG 579 then interacted. Whether this reflects a downstream consequence or compensatory adaptation to loss of PDE10A2 function is unclear. As stated, there are other isoforms of PDE10A that are found in the striatum. Because *Pde10a2* KO potentiated the ability of the PDE10A inhibitor AMG 579 to reduce DLS *Drd1* and *Drd2* expression, the results support the possibility that the striatal functional relevance of other PDE10A isoforms may be upregulated in *Pde10a2*-deficient mice. This again is consistent with reports that levels of striatal PDE10A1 were reportedly upregulated by 55% in *Pde10a2*$^{tTA/tTA}$ KO mutants [26] and also with the abundance of other striatal PDE10A isoforms that have been identified in humans [53,61].

Genotype-Dependent Changes in IEG Expression After Treatment with AMG 579

As with other PDE10A inhibitors like MP-10 and MR1916 [33,42], I predicted that treatment with AMG 579 would increase striatal IEG expression. However, the results showed the opposite. Treatment with the PDE10A inhibitor AMG 579 instead decreased *Fos* and *Egr1* expression in both the DLS and NAc. Here, contrary to what was seen with MSN markers, when genotypes were considered separately, AMG 579 elicited a significant decrease in IEG expression of WTs, with no significant change seen in *Pde10a2* KO mutants. In sum, the results

show that the dose of AMG 579 with promise to reduce 2-bottle choice intake of WT mice overall reduced DLS and NAc activation in WT mice, as indicated by *Egr1* and *Fos* expression, and these effects were not separately seen in *Pde10a2* KO mice.

Sex Differences in Treatment and Genotype Effect

I predicted that AMG 579 treatment and genotype effects would be more pronounced in male mice, however this generally was not the case. There were 3-way interaction trends involving *Drd2* expression in the DLS in which pairwise comparison revealed that AMG 579 reduced expression of *Drd2* in KO males more than female (mean z-score difference= -1.405) suggesting that the reduction effect seen as a result of *Pde10a2*-KO and AMG 579 is pronounced more in males vs. females. There was a significant sex difference in *Drd2* expression in the DLS of knockout mice that received the compound, in which the males had less *Drd2* expression than females. This seems to align with the hypothesis that the treatment and genotype effect would be more prominent in males. However, when looking at the data overall there does not seem to be a sex difference in expression of *Pde10a, Drd1,* or either of the IEGs.

The role of PDE10A2 in Problematic Ethanol Drinking in Ethanol-Dependent Mice

In a model of 2-bottle choice voluntary drinking in post-CIE mice that had undergone 6-8 cycles of chronic intermittent ethanol exposure, AMG 579 was able to significantly reduce ethanol consumption of WT post-CIE mice, but not in KO post-CIE mice (see Supplementary Figure 2). Thus, the ability of AMG 579 to reduce post-dependent drinking appears to be dependent on the PDE10A2 isoform, but the effect of AMG 579 to influence MSN marker expression in naïve mice does not. On the other hand, there are hints of this PDE10A2-dependent

pattern when looking at effects of AMG 579 on striatal IEG expression. That is, both in the DLS and NAc for *Fos* (Figure 1C-D) and in NAc for *Egr1* (Figure 1B), treatment with AMG 579 elicited significant and descriptively larger reductions in IEG expression in WT mice than in *Pde10a2*-KO mice. The results suggest that some of the inhibitor's effect to influence IEG activation is partly dependent on the PDE10A2 isoform. Overall, the findings suggest that insofar as AMG 579-induced changes in striatal IEG expression and post-dependent drinking were both *Pde10a2* dependent, they may relate to one another more than did the changes in MSN marker expression, which were less *Pde10a2* dependent.

Chapter 3: RNAscope to Measure *Drd1*, *Drd2*, and *Egr1* Activation in Rats

RNAscope is a method of fluorescent in-situ hybridization (FISH) that allows for labelling individual mRNA transcripts in a cell with a high level of specificity using fluorescent, molecularly-targeted probes. RNAscope involves individual RNA strands binding multiple Z-probe dimers that bind to a specific sequence of RNA on one side and the labeled probes on the other. Because the probes are attached to the individual RNA strand, the extent of normalized fluorescence observed semi-quantitatively relates to the degree of transcript expression (as opposed to the whole cell being marked) and one can estimate the relative quantity of RNA molecules that are positive for that probe to identify changes in relative cellular co-localization. By combining DAPI cellular staining with FISH estimates of standardized relative RNA expression, *Drd1*-positive vs. *Drd2*-positive cells can be identified to test if injection with AMG 579 is able to differentially increase (or reduce) activation of identified cell populations, and if it has a bias for one of those cell types. The potential changes in activation can be visualized to determine if there is bias towards any particular subregion in the striatum, the DMS, DLS, or NAc. The aim of this experiment is to see how injection with AMG 579 changes neuronal activation, as defined by *Egr1* expression, in *Drd1*- and *Drd2*-positive MSNs in three different brain regions – DLS, DMS, and the NAc – of male and female Wistar rats.

Studies show that when an instrumental behavior is acquired, including ethanol self-administration, its control is initially mediated by the nucleus accumbens [16], and the behavior is goal-directed and sensitive to changes in reinforcer outcome and incentive state. With greater experience with the behavior, the functional role of which compartment of the striatum subserves the behavior shifts first dorsally and becomes more associated with the DMS (with behavior still goal-directed), and then ultimately progresses laterally to the DLS. Once the behavior is under

DLS control, it tends to be outcome-insensitive behavior, which has been described as habit-like or compulsive-like [64]. This conceptual model suggests that PDE10A may be well-positioned to impact compulsive drinking, since it is highly expressed in the putamen and caudate nucleus regions, corresponding to the dorsal striatum [54]. This regional aspect of the control of goal-directed vs. pathological habit behavior is of interest and raises the question of whether anti-drinking doses of AMG 579 differentially influence MSNs within the NAc, DMS, or DLS subregions. I hypothesize to see a greater Treatment effect in the dorsal striatum (DLS and DMS) than in the nucleus accumbens, defined by greater MSN and IEG expression in the DLS and DMS than in the NAc after treatment with AMG 579, because the shift in region control of drinking behavior that biases the DLS during compulsive drinking.

I predict that I will see more D2-MSN activation compared to D1-MSN activation in the AMG 579-treated group, defined by greater *Egr1* expression in *Drd2*-positive cells because previous studies have shown PDE10A inhibition is linked to increased IEG expression in *Drd2*-expressing neurons compared to *Drd1*-expressing [32]. Similar to the previous chapter, it is expected that the Treatment effect will be more pronounced in the male rats than the females.

Prior experiments from my lab found a link between injection with AMG 579 in post-dependent chronic intermittent ethanol vapor-exposed male and female Wistar rats and reduced operant ethanol self-administration. The data from an unpublished manuscript from this lab [51] suggests that the highest dose of AMG 579 (444 nmol/kg, i.p.), in particular, significantly reduced ethanol intake compared to the vehicle control (pairwise comparison, $p<0.001$). Guided by these data, the 444 nmol/kg dose was determined to be the experimental group for this study. Because these data are currently unpublished, a summary graph of the relevant result is included below for Committee reference.

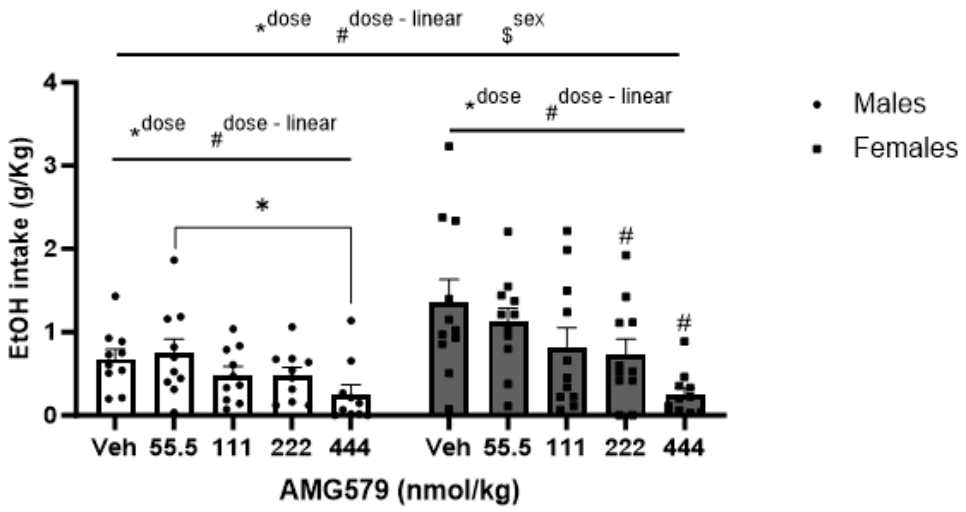

Supplemental Figure 1: Effects of AMG 579 pretreatment (~60 mins) on total EtOH intake in post-CIE male and female rats during 2-lever EtOH vs. water self-administration. Histograms show group M+SEM, and scatter shows the scores of individual subjects. N = 10-11/sex; *ANOVA within-subject effect; #ANOVA within-subject contrast; $ANOVA between-subject effect. Doses marked by the star sign differ significantly from the respective vehicle control. Doses marked by the star sign and a bracket differ significantly from each other. *, #, $ $p < 0.05$.

Chapter 3.1: Methods

Subjects:

Subjects for the RNAscope assay were used 18 (9/sex) adult (~3 months old) Wistar rats. Rats were maintained in a temperature- and humidity-controlled vivarium (see previous chapter) under a reverse dark light cycle (lights on 8pm, off 8am) with *ad libitum* access to food (Product Number: #7012, Teklad Diets) and tap water. All procedures conformed to the National Institutes for Health *Guide for the Care and Use of Animals* and were approved by the Institutional Animal Care and Use Committee of Scripps Research Institute.

Experimental Design and Tissue Collection

The study involved a 2 Treatment (AMG 579 vs. vehicle) X 2 Sex (Male vs. Female) X 3 Region (DLS vs. DMS vs. NAc) factorial design with Region as a within-subject factor. Rats were pseudo-randomly assigned to groups, matched for body weight. Rats were accustomed to the reversed-light cycle room for at least 2 weeks, during which they were handled and weighed regularly.

For the study, rats were intraperitonially injected with either AMG 579 (444 nmol/kg) or 10% HPBC vehicle dissolved in Nanopure water (1 ml/kg). They were then sacrificed by decapitation after being rapidly anesthetized with isoflurane 90 minutes after injection. After sacrifice, the brains were flash frozen using isopentane and dry ice, wrapped in aluminum foil, kept on dry ice post-dissection, and then stored in a -80 °C freezer. Brains were sliced at -20 °C using a cryostat coronally into 20 μm sections and mounted onto SuperFrost Plus slides (Fisher Scientific Catalog Number: 12-550-15). For the RNAscope assay, I assigned 2 sections at the A/P: +1.6-1.8 bregma coordinate per slide per animal.

RNAscope In Situ Hybridization

I conducted a 3-plex assay with the following gene targets assigned to the following probes: C1- *Drd1*; C2-*Drd2*; C3- *Egr1*. I hybridized the probes to the following fluorophores at the manufacture-recommended standard 1:1000 dilution- Channel 1: TSA Vivid Fluorophore 520 (green); Channel 2: TSA Vivid Fluorophore 570 (red); Channel 3: TSA Vivid Fluorophore 650 (far-red); and DAPI to stain cells. Following the protocol provided for "fresh frozen tissue" in the RNAscope Multiplex Fluorescent Reagent Kit v2 With Sample Preparation and Pretreatment User Manual provided by ACD (Document Number UM 323100). A negative and positive control probe was run in tandem with the 18 slides treated with *Drd1*, *Drd1*, and *Egr1* probes (20 slides total). All sections were analyzed in batch within the same single reaction to eliminate assay-to-assay variation.

Microscopy and Imaging

Slides were then imaged on a confocal microscope (Zeiss Confocal Laser-Scanning Microscope 780, 40× oil immersion, 2580 × 2580) where 2D snapshots of the DLS, DMS, and NAc for both hemispheres were taken. The different color channels for each image were merged and converted to .tiff using FIJI. Then a custom CellProfiler pipeline was used to count the expression levels within each DAPI-marked cell and colocalize *Drd1*, *Drd2*, and *Egr1* expression within each DAPI-stained cell.

Data Analysis

I took the $\log_{10}$ of the raw pixel counts for each gene target at the cell level and z-score standardized signal for each gene based on the expression level of the males that received

vehicle. Cells were either deemed *Drd1*-postive, *Drd2*-positve, or undetermined comparing 2 different threshold intensities for positive: 1) requiring any signal above 3 pixels that was the dominant expression or 2) requiring the dominant expression probe have a higher level of expression (z-score > 0), to increase confidence in the cell's positivity. I present results based on the second thresholding method based on its higher stringency for identifying cells labeled as *Drd1*- or *Drd2*-positve, but their significant differences identified were almost identical.

After determining which cells were *Drd1*- or *Drd2*-positive, the standardized signal intensity within the defined cell type (e.g., *Drd1* expression within *Drd1*-positive cells) and co-localized *Egr1* activation signal was then calculated. Standardized z-scores for each cell were then averaged on the image level and analyzed using a linear mixed model using SPSS with Sex, Treatment, and Region as factors. Region was a within-subject factor. Statistically significant interactions were defined as $p<0.05$.

Chapter 3.2 Results

Overall *Drd1*, *Drd2*, *Egr1* Expression Levels

As seen in Figure 4A, considering *Drd1* expression-levels across all DAPI-positive cell types, there was a significant three-way interaction between Treatment X Sex X Region [$F(2,104)=3.293$, $p=0.041$]. This reflected that in both males and females, AMG 579 significantly changed *Drd1* expression in the DMS, with an increase in expression in males but a decrease in females [males $F(1,104)=4.037$, $p=0.047$, females $F(1,104)=5.130$, $p=0.026$] compared to vehicle control. These effects did not reach significance in the NAc or DLS. Additionally, there was significantly higher expression of *Drd1* in the DMS of AMG 579-treated males than females [$F(1,104)=6.118$, $p=0.015$], whereas, conversely, vehicle-treated females tended to have greater DMS *Drd1* expression than their male counterparts [$F(1,104)=3.476$, $p=0.065$].

As Figure 4B shows, were no significant interactions or main effects in *Drd2* expression that were seen when region was used as a factor. However, when analyzing at the regions separately, in the DLS there was a Sex main effect whereby females expressed more *Drd2* than males [$F(1,39)=6.754$, $p=0.013$].

As seen in Figure 4C, analysis of *Egr1* expression in all DAPI-positive cells revealed Sex [$F(1,104)=8.214$, $p=0.005$] and Treatment [$F(1,104)=8.042$, $p=0.005$] main effects wherein males had higher *Egr1* expression and treatment with AMG 579 decreased *Egr1* expression. When analyzed by each region separately, the results showed that these main effects were driven by a Sex main effect in the NAc (males > females, $F(1,28)=7.880$, $p=0.009$) as well as Treatment [$F(1,37)=8.550$, $p=0.006$] and a 2-way Treatment X Sex interaction in the DMS. Thus, in the DMS, males that received vehicle had higher *Egr1* expression levels than females with the same

treatment [F(1,37)=5.961, p=0.020], and AMG 579 decreased DMS *Egr1* expression of male rats [F(1,37)=17.619, p<0.001] vs. vehicle control. However, there were no significant Region main effects or interaction in the model.

Drd1 and *Egr1* Expression Levels in *Drd1*-expressing cells

There were no significant main or interaction effects in the *Drd1* expression levels within the *Drd1*-expressing cells (Figure 5A).

As Figure 5B shows, *Egr1* expression levels had a significant 3-way interaction between Treatment X Region X Sex [F(2,103)=3.682, p=0.029]. This reflected that in the DMS of the males, AMG 579 reduced the expression of *Egr1* [F(1,103)=7.668, p=0.007] vs. vehicle control. In females treated with vehicle, DLS had more *Egr1* expression than NAc [F(2,103)=2.525, p=0.032]. In males treated with AMG 579, the DLS had significantly higher expression than the DMS [F(2,103)=5.189, p=0.002]. In the DMS of rats that received drug, females had higher *Egr1* expression than males [F(2,103)=2.525, p=0.044]. When analyzing each region separately, that the results show that in the NAc there was a Sex main effect whereby males showed higher *Egr1* expression [F(1,27)=6.084, p=0.020] and in DMS there was a 2-way interaction between Treatment X Sex [F(1,37)=5.331, p=0.027] where in rats that received vehicle treatment, males showed higher *Egr1* expression than females [F(1,37)=5.354, p=0.026]. AMG 579 reduced *Egr1* expression of males in the NAc as compared with vehicle controls. However, there were no Region main effects or interaction in the model.

Drd2 and *Egr1* Expression Levels in *Drd2*-expressing cells

As Figure 6A shows, there was a Sex main effect on *Drd2* expression in *Drd2*-expressing cells in which females showed significantly higher *Drd2* expression than males [$F(1,104)=4.520$, $p=0.036$]. When each region was analyzed separately, the results suggest that this sex difference was driven by the DLS [$F(1,39)=6.793$, $p=0.013$], as none of the other regions show significant sex differences in *Drd2* expression within *Drd2* positive cells. However, there were no Treatment or Region main effects or interactions in the overall model.

As seen in Figure 6B, *Egr1* expression within *Drd2*-positive cells showed both Sex and Treatment main effects, whereby males had higher expression of *Egr1* [$F(1,104)=10.112$, $p=0.002$], and treatment with AMG 579 reduced expression of *Egr1* [$F(1,104)=8.308$, $p=0.005$]. Considering each region separately, there was a 2-way (Treatment X Sex) interaction in the DMS [$F(1,37)=7.558$, $p=0.009$], whereby AMG 579-treated males had higher *Egr1* expression than females with same treatment [$F(1,37)=4.640$, $p=0.038$]. However, in the overall mixed model, there were no main effects or interactions involving Region.

Drd1, *Drd2*, and *Egr1* Expression Levels in Undefined Cells.

As Figure 7A shows, *Drd1* expression within undefined cells showed a significant 3-way Treatment X Sex X Region [$F(2,104)=3.549$, $p=0.032$]. Treatment with AMG 579 decreased *Drd1* expression in the DMS of female rats [$F(1,104)=5.381$, $p=0.022$], but not in the male rats. Consequently AMG 579-treated male rats showed significantly higher DMS *Drd1* expression than their female counterparts [$F(1,104)=5.213$, $p=0.024$]. Conversely, vehicle-treated females showed greater DMS *Drd1* than males [$F(1,104)=4.119$, $p=0.045$].

As Figure 7B shows, *Drd2* expression showed a Sex main effect in which females had higher *Drd2* expression than males [$F(1,104)=4.018$, $p=0.048$]. There were no main or interaction effects involving Treatment or Region.

Lastly, as Figure 7C shows, *Egr1* expression in undefined cells showed Treatment, Sex, and Region main effects. Specifically, AMG 579 reduced expression of *Egr1* [$F(1,104)=8.513$, $p=0.004$], males had higher *Egr1* than females [$F(1,104)=10.123$, $p=0.002$], and the undefined cells in the DLS had higher *Egr1* expression than those in the DMS [$F(1,104)=3.486$, $p=0.034$].

Chapter 3.3 Discussion

Similar to Chapter 2 studies in mice, the way AMG 579 influenced MSN marker expression, IEG expression, and their co-expression in rats was different than what was expected. As in Chapter 2, AMG 579 unexpectedly reduced *Egr1* expression, seen broadly in *Drd2*-, but not *Drd1*-, expressing cells. When looking at regional differences, greater treatment-related effects were seen within the dorsal striatum. For example, expression-levels of *Drd1* across all DAPI-positive cell types showed significance at the 3-way Treatment X Sex X Region level. This was because AMG 579 selectively reduced *Drd1* expression in the DMS. Within this region, males normally showed lower *Drd1* expression than females, a sex difference that reversed with AMG 579 treatment. AMG 579 also decreased *Egr1* expression in DAPI-positive cells, but there seemed to be cell type variation in this effect. Specifically, in *Drd1*-positve cells AMG 579 differentially reduced *Egr1* expression in the DLS of males, whereas it reduced *Egr1* expression more broadly in *Drd2*-positive and undefined cells. Lastly, in undefined cells, treatment with AMG 579 decreased *Drd1* expression in the DMS of female rats, but not male rats.

Regional Differences in AMG 579 Treatment Effects on MSN expression

I hypothesized to see a stronger Treatment effect in the AMG 579 treated group, defined by greater changes in MSN marker and IEG expression, within the dorsal striatum than in the nucleus accumbens. Such an outcome may have potential therapeutic implications for modulating the regional shift in control of behavior associated with the development of compulsive drinking. Consistent with this, there were 3-way interactions involving Treatment and Region for AMG 579 effects on *Egr1* and *Drd1* expression (*Drd1* expression in all DAPI-

positive cells, *Egr1* expression in *Drd1*-positive cells, *Drd1* expression in undefined cells) that suggest a differential impact of AMG 579 administration on the dorsal striatum. Regarding *Drd1* expression within the undefined cells, there was a larger AMG 579 treatment effect within the DMS of females than in the other 2 regions. The 3-way effect in *Egr1* expression in *Drd1*-positive cells saw a Treatment effect in the DMS and in *Drd1* expression in all DAPI-positive cells, there was a Treatment effect in the DMS of both male and female rats. Generally, Treatment effects were seen as a decrease in expression, similar to the results seen in Chapter 2, with the exception of *Drd1* expression in all DAPI positive cells in DMS of males where there was an increase in expression after treatment with AMG 579. This seems to support the hypothesis that AMG 579 differentially affected the dorsal striatum, the DMS especially, more than the NAc.

Cell-type differences in AMG 579 Treatment Effects on *Egr1* Expression: *Drd1*- vs. *Drd2*-Positive Cells

I predicted that there would be more D2 activation compared to D1 activation in the AMG 579-treated group, defined by greater *Egr1* expression in *Drd2*-positive cells. What I instead saw was that *Egr1* expression in *Drd2*-positive cells was significantly lower in the AMG 579 treated group than the vehicle treated. However, there was no significant effect of AMG 579 on the expression of *Egr1* in *Drd1*-positive cells. This seems to partially agree with the hypothesis insofar that the Treatment effect was more pronounced in the *Drd2*-positive cells than in the *Drd1*-positive cell populations. However, this effect was an unexpected decrease in IEG expression, which nonetheless seems to align with my findings from the previous chapter. In previous studies, it was shown that the PDE10A inhibitor, MP-10, induced greater IEG activation in D2 cells more than D1 cells. AMG 579 seems to have a similar indirect pathway-

related effect, but in the opposite direction, whereby it decreased IEG expression in D2 cells more significantly than in D1 cells.

Sex Differences in AMG 579 Treatment Effect on *Drd1* and *Egr1* Expression

Similar to the previous chapter, treatment with AMG 579 treatment was expected to be more pronounced in the male rats than the females. However, what was seen was that treatment with AMG 579 altered expression *Drd1* and *Egr1* in opposing directions between the sexes. For example, in *Drd1* expression in DAPI-positive cells revealed that in DMS of males, there was increased expression as a result of AMG 579 treatment but in females there was the opposite effect where there was decreased expression after treatment with AMG 579. In the same region, males saw a decrease in *Egr1* expression in *Drd1*-postive cells, with no significant effect in females. In contrast, *Drd1* expression in undefined cells decreased in females with no effect seen in males. This suggests that AMG 579 has a sexually dimorphic effect in the DMS that varies by gene target or cell type.

Chapter 4: Conclusion

Chronic ethanol exposure and consumption can lead to maladaptive neurobiological changes in the brain's reward and motivation systems and perpetuate harmful drinking. A proposed mechanism for this is that chronic alcohol may disrupt balance between the D1-direct and D2-indirect pathways that lead to relatively underactive iMSNs or overactive dMSNs and compulsive drinking. I investigated the ability of the ethanol drinking-relevant doses on the drug-candidate AMG 579 to affect D1 and D2 MSN activation. In Chapter 2, I used qPCR to measure the change in expression levels in the D1 MSN markers *Drd1* and the D2 MSN markers *Drd2* and *Penk* as well as changes in markers of neuronal activation, *Egr1* and *Fos*. Wild-type and PDE10A2$^{tTA/tTA}$ mice were administered a dose of AMG 579 at a dose that reduces EtOH consumption in post-dependent mice (100 nmol/kg, i.p.) and then after a 90-minute post-treatment interval, brain punches of the DLS and NAc were taken. The mRNA was extracted and reverse transcribed before conducting qPCR on the following gene targets: *Pde10a2*, *Egr1*, *Fos*, *Drd1*, *Drd2*, *Penk*. Results showed that both *Pde10a2*-knockout and treatment with AMG 579 reduced *Drd1* and *Drd2* and *Pde10a2* expression. *Penk* expression was reduced in the knockout mice as a result of the AMG 579 compound as well. Even though the statistical analysis showed that AMG 579 reduced *Egr1* and *Fos* expression regardless of genotype, descriptively there was less of a significant effect in the KO mice, but this could be due to small sample size and the limits of power associated with that. Because of the limitation of the sample size, the experiment would need to be expanded with a larger sample size in order to increase confidence in this provisional interpretation that AMG 579 had a blunted effect has on IEG expression in the male KO mice.

In Chapter 3, RNAscope was used to see if injection with AMG 579 differentially activated D1- or D2-positive cell types, and if these effects differed by region or sex. I conducted RNAscope on wild-type, alcohol naive adult Wistar rats. Firstly, I treated them with a dose that has previously shown to decrease ethanol drinking in post-CIE rats (444 nmol/kg, i.p.), and after a 90-minute post-injection period, extracted their brains which were flash frozen. The brains were sectioned using a cryostat and mounted on slides. Slides in the A/P: +1.6-1.8 bregma range were selected for the RNAscope assay. I conducted the assay using the protocol provided by ACD for fresh frozen tissue using probes for *Drd1*, *Drd2*, and *Egr1*. The DLS, DMS, and NAc were imaged using a confocal microscope, and the puncta were counted using a custom CellProfiler pipeline. D1, D2, and undefined cells were defined by thresholding the standardized *Drd1* and *Drd2* expression. In all three cell groups (D1, D2, and undefined), treatment with AMG 579 reduced expression of *Egr1*. Effects were more significant in the DMS and DLS than in the NAc. Treatment seemed to have a sexually dimorphic effect in the DMS that varied by gene target or cell type.

The effects of this compound were different than what was hypothesized. Other PDE10A inhibitors, like MP-10, MR1916, and TAK-063 seem to activate both D1 and D2 marker expression; however, here, both the qPCR and RNAscope results appeared to show that the compound decreased both *Drd1*- and *Drd2*-mediated cell expression and IEG activation. These results were consistent with the changes seen in the KO mice, suggesting that AMG 579 also reduces expression in a manner consistent with *Pde10a2*-KO. Even though the statistical analysis showed that the compound has an effect on IEG expression regardless of genotype, descriptively there was no significant effect in the KO male mice, suggesting a dependence on the *Pde10a2*

isoform. Because of the limitation of small sample size, this experiment would need to be repeated with a larger sample size in order to increased confidence in this tentative conclusion.

Preliminary results (see Supplementary Figure 2) suggest that higher AMG 579 doses (200 nmol/kg) have the potential to reduce ethanol drinking in WT, but not KO, post-CIE exposure mice. Further study is needed to see how MSN marker (especially *Pde10a2*) and IEG expression changes as a result of CIE exposure and how AMG 579 through a range of doses influences expression in post-CIE mice.

Further study with a larger sample size is needed to confirm the deactivation effect AMG 579 has on MSN marker expression. There still needs to be more research looking at how the compound affects expression levels in alcohol dependent animals as well as if there is a change in how the compound affects marker expression in high- vs. low-drinking animals since MR1916 was shown to have different effects on expression depending on whether the animals were high or low drinkers. The response to PDE10A inhibition might change as a result of alcohol-exposure as well, so testing the response the compound has on alcohol-exposed mice in the future is vital to understanding how this compound works. It is also unknown if a treatment that focuses on reducing overactive D1 expression is better suited to treat AUD then one that increases the expression of underactive D2 expression, further study is needed to determine if this reduction is more preferential or effective. It would be interesting to compare AMG 579, which potentially reduces ethanol consumption by reducing D1 expression with a PDE10A inhibitor that acts on increasing D2 expression to see which one is better suited to modulate problematic drinking and to compare the changes in MSN marker and IEG expression at equimolar doses.

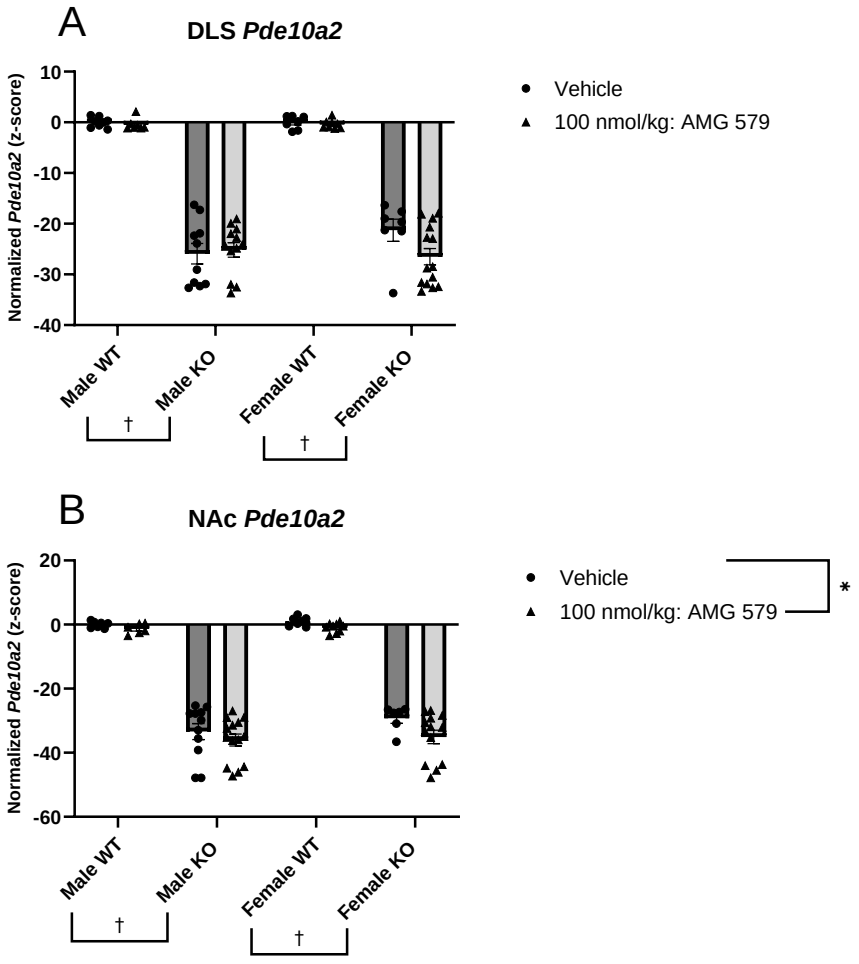

Figure 1: Effects of AMG 579 on gene expression of phosphodiesterase 10a2 (*Pde10a2*) in the (A) dorsal–lateral striatum and (B) nucleus accumbens in EtOH-naïve male and female *Pde10a2*-KO and Wild-type mice 90 minutes after injection (i.p.) with AMG 579 (100 nmol/kg) or 10% *w/v* 4-hydroxypropyl-β-cyclodextrin (vehicle). Each bar represents the mean z-score ± SEM, showing individual values. *N*= 6–14/treatment/sex. *=significantly different Treatment main effect, †= significantly different Genotype main effect. *, † $p < 0.05$

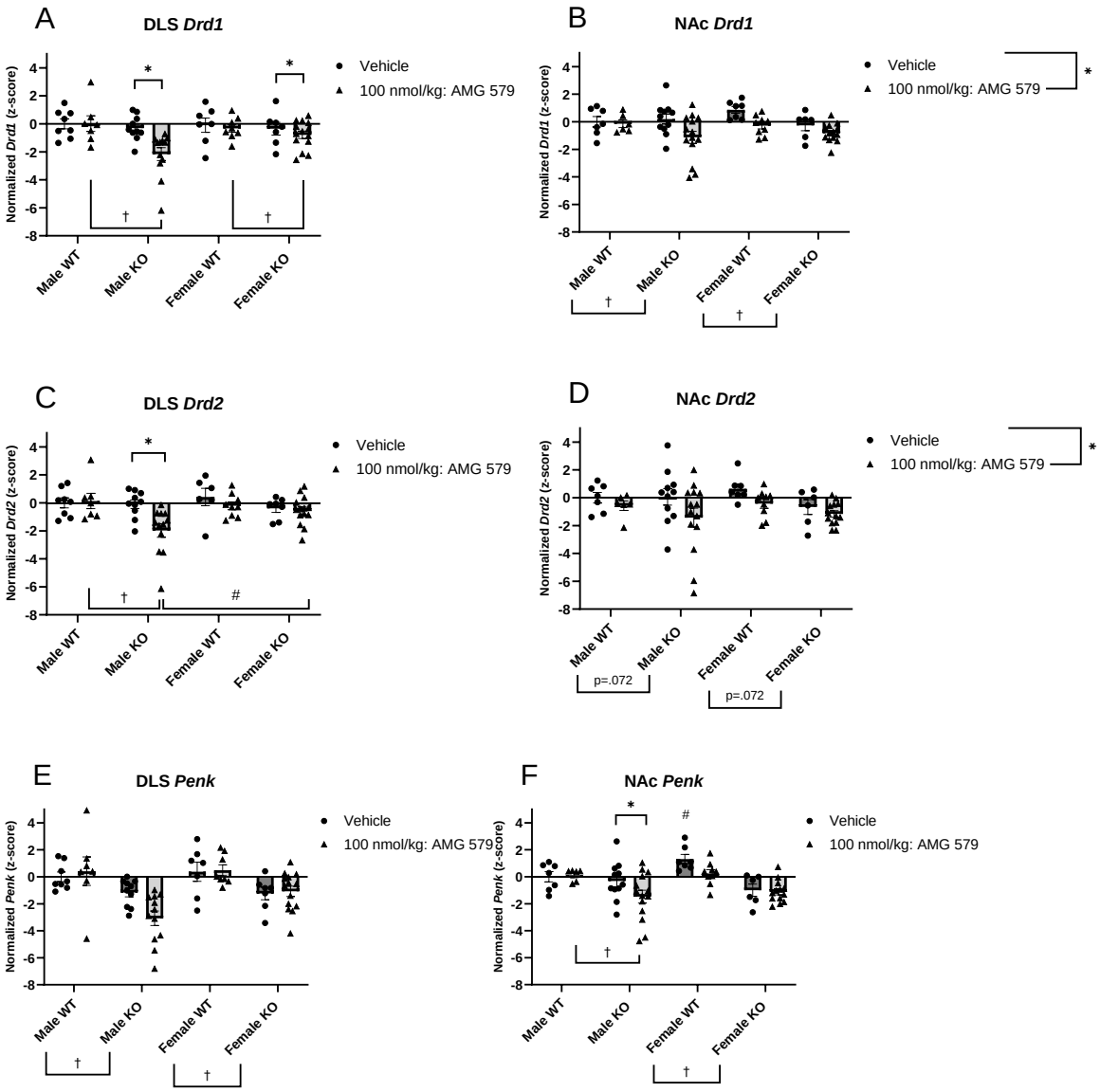

Figure 2: Figure 2. Effects of AMG 579 on gene expression of Medium Spiny Neuron (MSN) Markers: (A-B) dopamine receptor 1 (*Drd1*), (C-D) dopamine receptor 2 (*Drd2*), (E-F) enkephalin (*Penk*) in the (A,C,E) dorsal–lateral striatum and (B,D,F) nucleus accumbens in EtOH-naïve male and female *Pde10a2*-KO and WT mice 90 minutes after injection (i.p.) with AMG 579 (100 nmol/kg) or 10% *w/v* 4-hydroxypropyl-β-cyclodextrin (vehicle). Each bar represents the mean z-score ± SEM, showing individual values. *N*= 6–14/treatment/sex. *=significantly different Treatment effect, #= significantly different Sex effect, †= significantly different Genotype effect. *, #, † $p < 0.05$

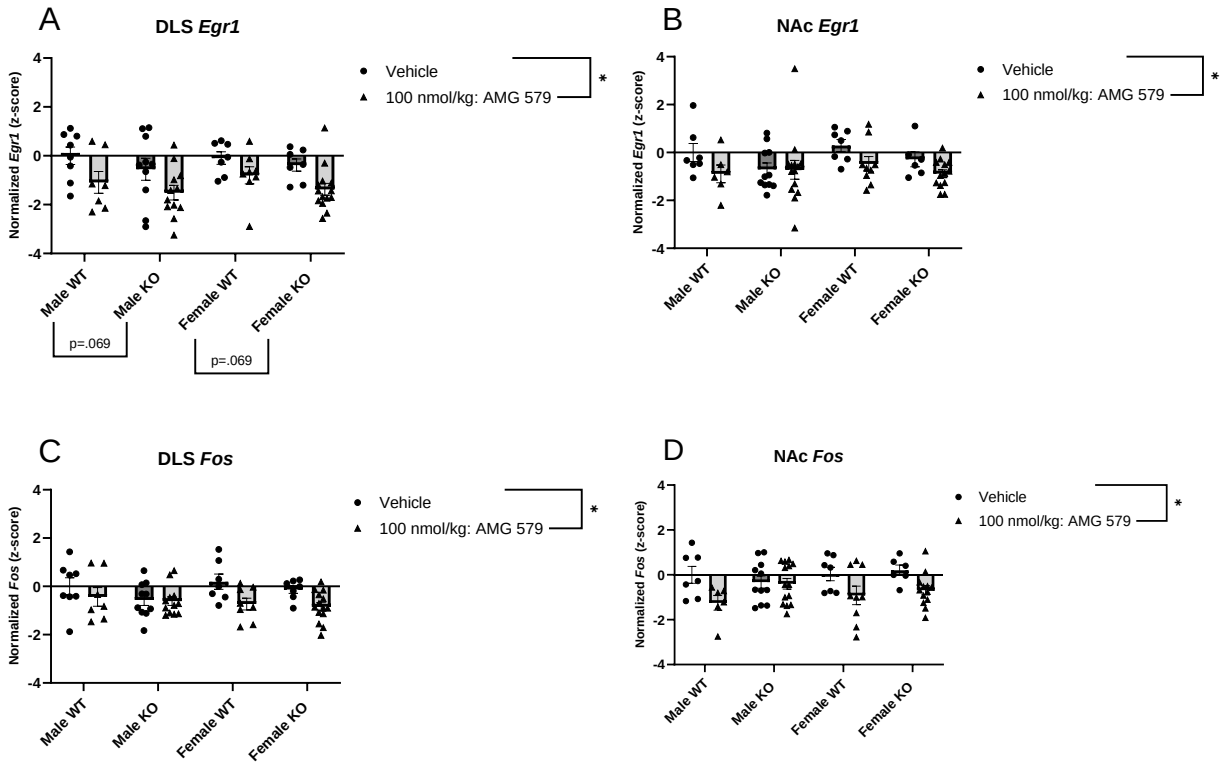

Figure 3: Effects of AMG 579 on gene expression of Immediate Early Genes (IEGs): (A-B) early growth response protein 1 (*Egr1*), (C-D) FBJ murine osteosarcoma viral oncogene homolog (*Fos*) in the (A,C) dorsal–lateral striatum and (B,D) nucleus accumbens in EtOH-naïve male and female *Pde10a2*-KO and WT mice 90 minutes after injection (i.p.) with AMG 579 (100 nmol/kg) or 10% *w/v* 4-hydroxypropyl-β-cyclodextrin (vehicle). Each bar represents the mean z-score ± SEM, showing individual values. *N*= 6–14/treatment/sex. *=significant Treatment effect, $p < 0.05$.

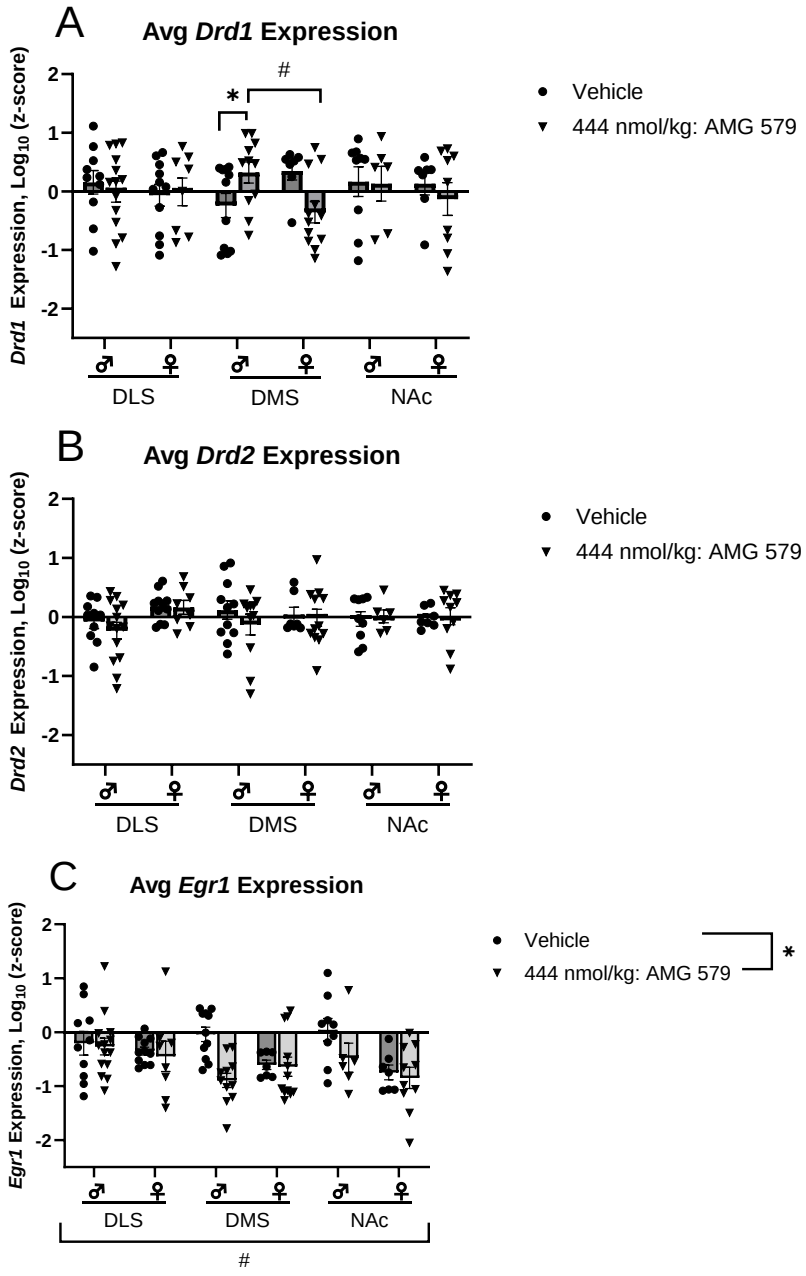

Figure 4: Effects of AMG 579 on (A) dopamine receptor 1 (*Drd1*), (B) dopamine receptor 2 (*Drd2*), and (C) early growth response protein 1 (*Egr1*) gene expression in DAPI-positive cells, regardless of cell type, in the dorsal-lateral striatum (DLS), dorsal-medial striatum (DMS), and nucleus accumbens (NAc) of male and female EtOH-naïve Wistar rats 90 mins after injection (i.p.) with AMG 579 (444 nmol/kg) or 10% *w/v* 4-hydroxypropyl-β-cyclodextrin (vehicle). Each bar represents the mean z-score ± SEM, showing individual values. *N*= 6-14 /treatment/sex/region. *=significantly different Treatment effect, #= significantly different Sex effect. *, # $p < 0.05$

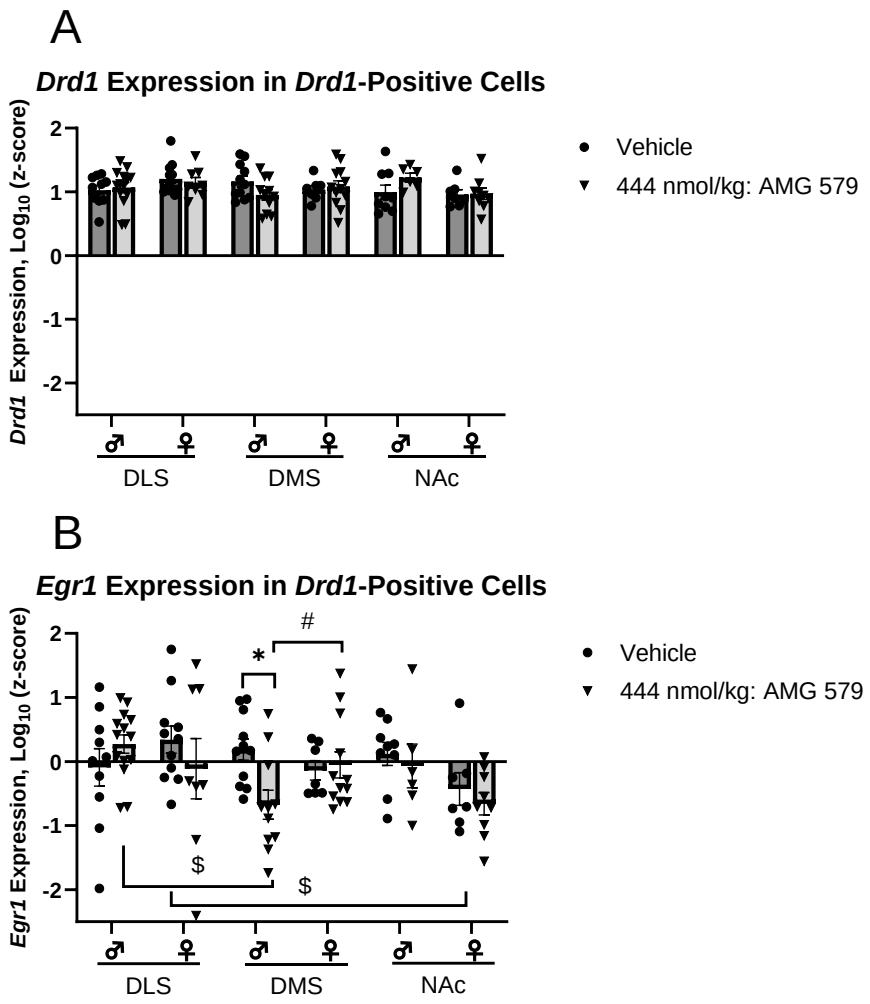

Figure 5: Effects of AMG 579 on of (A) dopamine receptor 1 (*Drd1*), and (B) early growth response protein 1 (*Egr1*) gene expression in *Drd1*-positive cells in the dorsal-lateral striatum (DLS), dorsal-medial striatum (DMS), and nucleus accumbens (NAc) in male and female EtOH-naïve Wistar rats 90 mins after injection (i.p.) with AMG 579 (444 nmol/kg) or 10% *w/v* 4-hydroxypropyl-β-cyclodextrin (vehicle). Each bar represents the mean z-score ± SEM, showing individual values. *N*= 7–14/treatment/sex/region. *=significantly different Treatment effect, #= significantly different Sex effect, $=significantly different Region effect.
*, #, $ $p < 0.05$

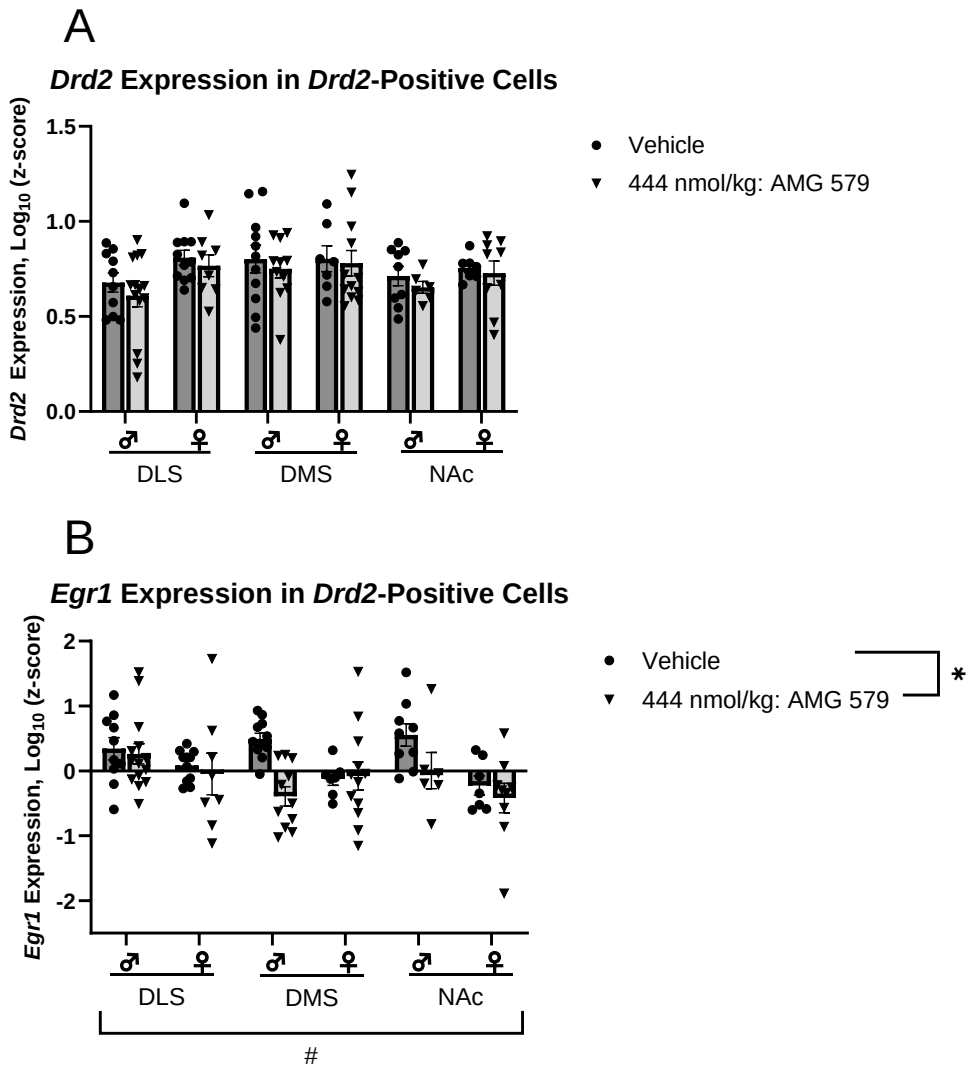

Figure 6: Effects of AMG 579 on (A) dopamine receptor 2 (*Drd2*), and (B) early growth response protein 1 (*Egr1*) gene expression in *Drd2*-positive cells in the dorsal-lateral striatum (DLS), dorsal-medial striatum (DMS), and nucleus accumbens (NAc) in male and female EtOH-naïve Wistar rats 90 mins after injection (i.p.) with AMG 579 (444 nmol/kg) or 10% *w/v* 4-hydroxypropyl-β-cyclodextrin (vehicle). Each bar represents the mean z-score ± SEM, showing individual values. *N*= 6–14/treatment/sex/region. *=significantly different Treatment effect, #= significantly different Sex effect. *, # $p < 0.05$

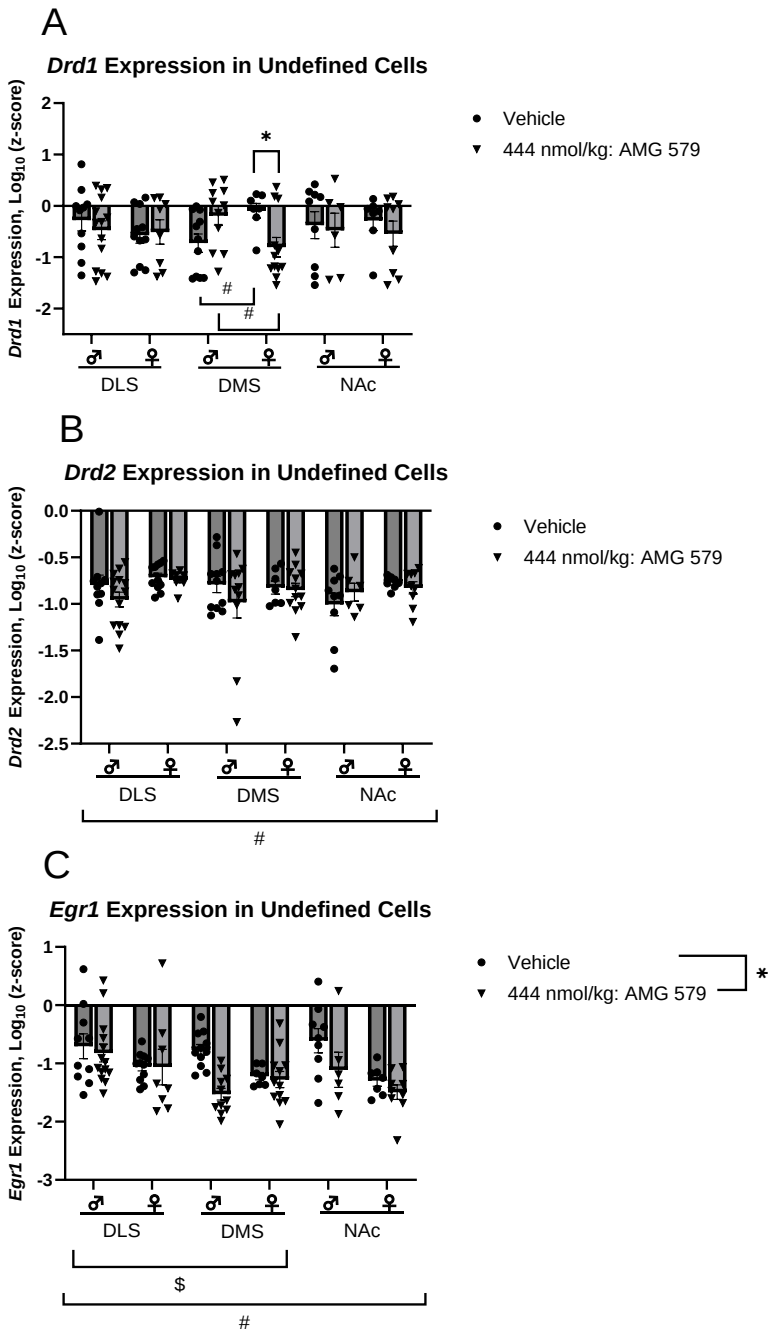

Figure 7: Effects of AMG 579 on of (A) dopamine receptor 1 (*Drd1*), (B) dopamine receptor 2 (*Drd2*), and (C) early growth response protein 1 (*Egr1*) gene expression in undefined cell-type in the dorsal-lateral striatum (DLS), dorsal-medial striatum (DMS), and nucleus accumbens (NAc) in male and female EtOH-naïve Wistar rats 90 mins after injection (i.p.) with AMG 579 (444 nmol/kg) or 10% *w/v* 4-hydroxypropyl-β-cyclodextrin (vehicle). Each bar represents the mean z-score ± SEM, showing individual values. *N*= 6–14/treatment/sex/region. *=significantly different Treatment effect, $=significantly different Region effect, #= significantly different Sex effect. *, #, $ $p < 0.05$

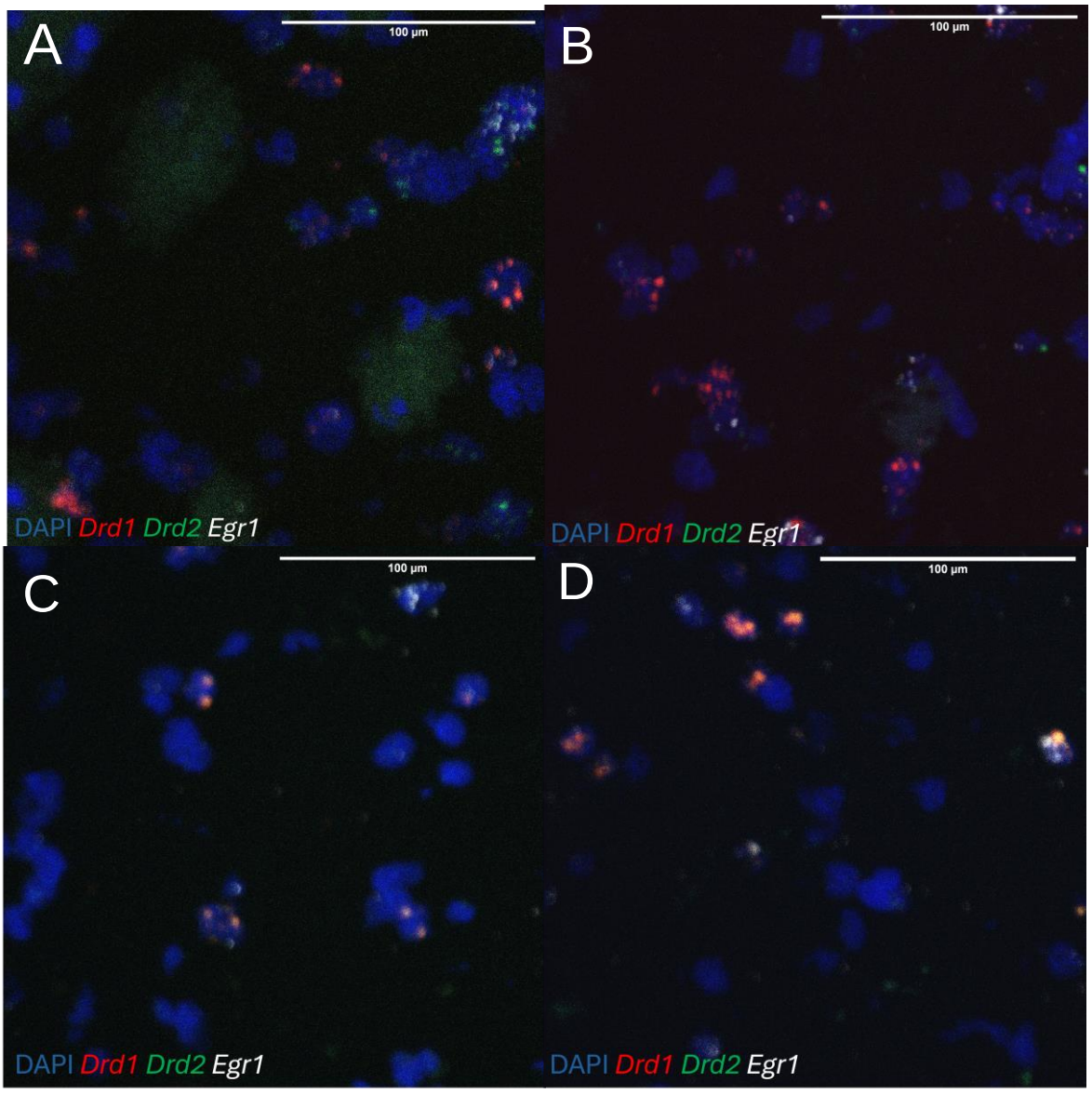

Figure 8: Confocal microscopy images of typical dorsal-medial striatum coronal section studied with RNAscope fluorescent in-situ hybridization from (A) vehicle-treated female (B) AMG 579-treated female (444 nmol/kg, i.p.) (C) vehicle-treated male (D) AMG 579-treated male (444 nmol/kg, i.p.) Wistar rats 90 min after administration. Representative of the significant ($p< 0.05$) difference of *Egr1* expression in *Drd1*-expressing cells. 2-way Treatment X Sex interactions: mean z-score difference of treated females – males = 0.622 and AMG 579 treated males – control males mean z-score difference = -0.863. Vehicle treated female panel (A) represents median *Egr1* expression for that group (z-score = 0.358)

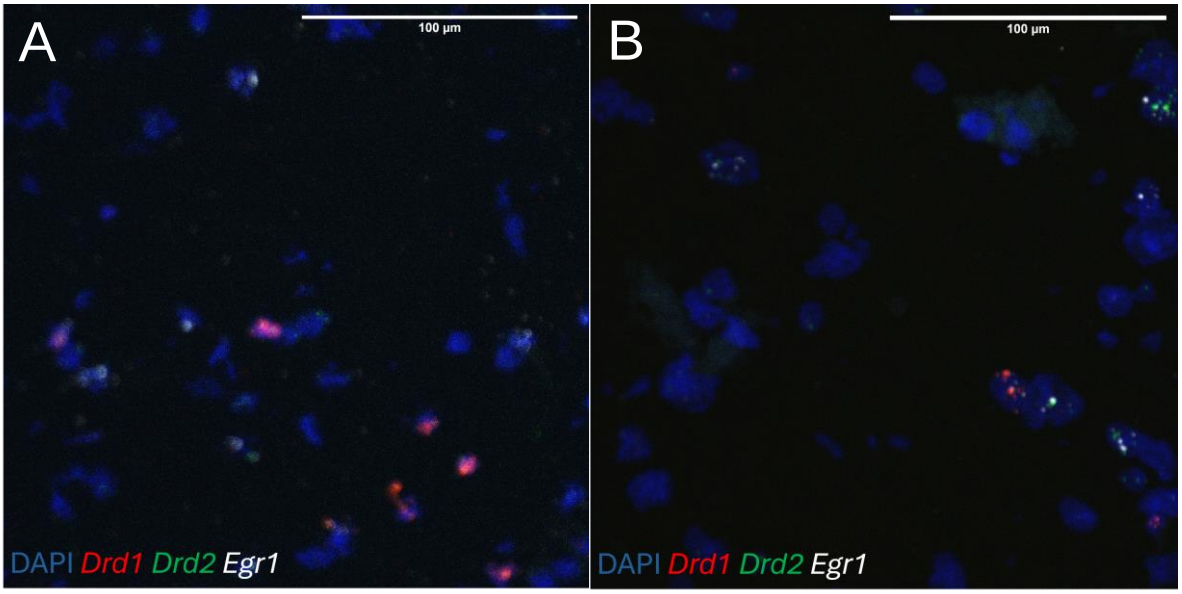

Figure 9: Confocal microscopy images of typical nucleus accumbens coronal section studied with RNAscope fluorescent in-situ hybridization from (A) AMG 579-treated male (444 nmol/kg, i.p.) (B) AMG 579-treated female (444 nmol/kg, i.p.) Wistar rats 90 min after administration. Representative of the significant ($p< 0.05$) Sex main effect reflected in the mean difference of *Egr1* z-scores in *Drd1*-expressing cells: Males - Females mean z-score difference= 0.569.

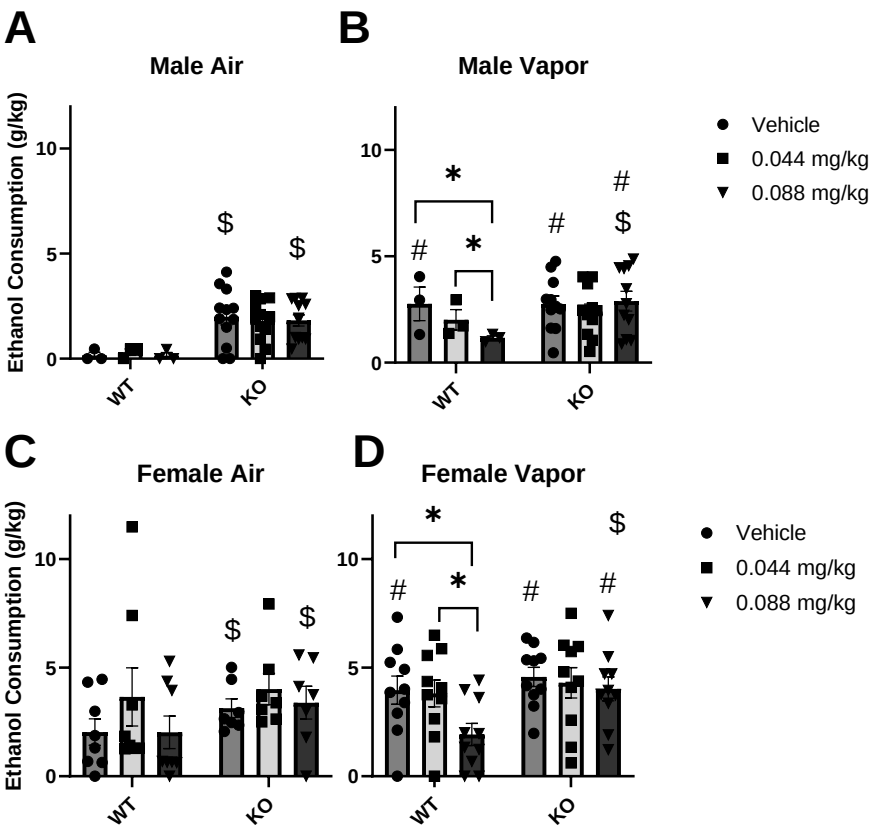

Supplemental Figure 2: Effects of AMG 579 pretreatment (~60 min, i.p.) on total EtOH intake in post-CIE (B,D) and air control (A,C) male (A-B) and female (C-D) mice during 2-bottle choice EtOH vs. water self-administration. Data collected by Scripps Animal Models Core. Histograms show group *M*+SEM, with scatter plots showing individual values. *N*=3-12 /sex/genotype. *= doses differ significantly from each other, $= dose differs significantly from respective WT control, #= dose differs significantly from air control. *, $, #, $p < 0.05$ using repeated measures mixed model with Dose as within-subject factors and Genotype, Air, and Sex as between-subject factors.

REFERENCES

1. Grant BF, Goldstein RB, Saha TD, Chou SP, Jung J, Zhang H, Pickering RP, Ruan WJ, Smith SM, Huang B, Hasin DS. Epidemiology of DSM-5 Alcohol Use Disorder: Results From the National Epidemiologic Survey on Alcohol and Related Conditions III. JAMA Psychiatry. 2015 Aug 1;72(8):757–66.

2. Stinson FS, Grant BF, Dawson DA, Ruan WJ, Huang B, Saha T. Comorbidity between DSM-IV alcohol and specific drug use disorders in the United States: Results from the National Epidemiologic Survey on Alcohol and Related Conditions. Drug and Alcohol Dependence. 2005 Oct 1;80(1):105–16.

3. Kendler KS, Ohlsson H, Sundquist J, Sundquist K. Alcohol Use Disorder and Mortality Across the Lifespan: A Longitudinal Cohort and Co-relative Analysis. JAMA Psychiatry. 2016 Jun 1;73(6):575–81.

4. Holt SR, Tobin DG. Pharmacotherapy for Alcohol Use Disorder. Medical Clinics of North America. 2018 Jul 1;102(4):653–66.

5. Dawson DA, Goldstein RB, Grant BF. Rates and Correlates of Relapse Among Individuals in Remission From DSM-IV Alcohol Dependence: A 3-Year Follow-Up. Alcoholism: Clinical and Experimental Research. 2007;31(12):2036–45.

6. Ozluk P, Cobb R, Sylwestrzak G, Raina D, Bailly E. Alcohol-Attributable Medical Costs in Commercially Insured and Medicaid Populations. AJPM Focus. 2022 Dec 1;1(2):100036.

7. Sacks JJ, Gonzales KR, Bouchery EE, Tomedi LE, Brewer RD. 2010 National and State Costs of Excessive Alcohol Consumption. American Journal of Preventive Medicine. 2015 Nov 1;49(5):e73–9.

8. Maia TV, Frank MJ. From reinforcement learning models to psychiatric and neurological disorders. Nat Neurosci. 2011 Feb;14(2):154–62.

9. LeBlanc KH, London TD, Szczot I, Bocarsly ME, Friend DM, Nguyen KP, Mengesha MM, Rubinstein M, Alvarez VA, Kravitz AV. Striatopallidal neurons control avoidance behavior in exploratory tasks. Mol Psychiatry. 2020 Feb;25(2):491–505.

10. Spigolon G, Fisone G. Signal transduction in l-DOPA-induced dyskinesia: from receptor sensitization to abnormal gene expression. J Neural Transm. 2018 Aug 1;125(8):1171–86.

11. Girault JA, Greengard P, Nairn AC. Chapter 29 - Regulation of Striatal Signaling by Protein Phosphatases. In: Steiner H, Tseng KY, editors. Handbook of Behavioral Neuroscience [Internet]. Elsevier; 2016 [cited 2024 Feb 17]. p. 583–607. (Handbook of Basal Ganglia Structure and Function, Second Edition; vol. 24). Available from: https://www.sciencedirect.com/science/article/pii/B9780128022061000295

12. Cheng Y, Huang CCY, Ma T, Wei X, Wang X, Lu J, Wang J. Distinct Synaptic Strengthening of the Striatal Direct and Indirect Pathways Drives Alcohol Consumption. Biological Psychiatry. 2017 Jun 1;81(11):918–29.

13. Barker JM, Corbit LH, Robinson DL, Gremel CM, Gonzales RA, Chandler LJ. Corticostriatal circuitry and habitual ethanol seeking. Alcohol. 2015 Dec 1;49(8):817–24.

14. Shin JH, Kim D, Jung MW. Differential coding of reward and movement information in the dorsomedial striatal direct and indirect pathways. Nat Commun. 2018 Jan 26;9(1):404.

15. Park K, Volkow ND, Pan Y, Du C. Chronic Cocaine Dampens Dopamine Signaling during Cocaine Intoxication and Unbalances D1 over D2 Receptor Signaling. J Neurosci. 2013 Oct 2;33(40):15827–36.

16. Giuliano C, Belin D, Everitt BJ. Compulsive Alcohol Seeking Results from a Failure to Disengage Dorsolateral Striatal Control over Behavior. J Neurosci. 2019 Feb 27;39(9):1744–54.

17. Loughney K, Snyder PB, Uher L, Rosman GJ, Ferguson K, Florio VA. Isolation and characterization of PDE10A, a novel human 3′, 5′-cyclic nucleotide phosphodiesterase. Gene. 1999 Jun 24;234(1):109–17.

18. Soderling SH, Bayuga SJ, Beavo JA. Isolation and characterization of a dual-substrate phosphodiesterase gene family: PDE10A. Proceedings of the National Academy of Sciences. 1999 Jun 8;96(12):7071–6.

19. Ramirez AD, Smith SM. Regulation of Dopamine Signaling in the Striatum by Phosphodiesterase Inhibitors: Novel Therapeutics to Treat Neurological and Psychiatric Disorders. Central Nervous System Agents in Medicinal Chemistry. 2014;14(2):72–82.

20. Bell RL, Lopez MF, Cui C, Egli M, Johnson KW, Franklin KM, Becker HC. Ibudilast reduces alcohol drinking in multiple animal models of alcohol dependence. Addiction Biology. 2015;20(1):38–42.

21. Grodin EN, Bujarski S, Towns B, Burnette E, Nieto S, Lim A, Lin J, Miotto K, Gillis A, Irwin MR, Evans C, Ray LA. Ibudilast, a neuroimmune modulator, reduces heavy drinking and alcohol cue-elicited neural activation: a randomized trial. Transl Psychiatry. 2021 Jun 12;11(1):355.

22. Kotera J, Fujishige K, Omori K. Immunohistochemical Localization of cGMP-binding cGMP-specific Phosphodiesterase (PDE5) in Rat Tissues. J Histochem Cytochem. 2000 May 1;48(5):685–93.

23. Kass DA, Champion HC, Beavo JA. Phosphodiesterase Type 5. Circulation Research. 2007 Nov 26;101(11):1084–95.

24. Russwurm C, Koesling D, Russwurm M. Phosphodiesterase 10A Is Tethered to a Synaptic Signaling Complex in Striatum*. Journal of Biological Chemistry. 2015 May 8;290(19):11936–47.

25. Polito M, Guiot E, Gangarossa G, Longueville S, Doulazmi M, Valjent E, Hervé D, Girault JA, Paupardin-Tritsch D, Castro LRV, Vincent P. Selective Effects of PDE10A Inhibitors on Striatopallidal Neurons Require Phosphatase Inhibition by DARPP-32. eNeuro [Internet]. 2015 Jul 1 [cited 2024 Feb 16];2(4). Available from: https://www.eneuro.org/content/2/4/ENEURO.0060-15.2015

26. Sano H, Nagai Y, Miyakawa T, Shigemoto R, Yokoi M. Increased social interaction in mice deficient of the striatal medium spiny neuron-specific phosphodiesterase 10A2. J Neurochem. 2008 Apr;105(2):546–56.

27. MacMullen CM, Vick K, Pacifico R, Fallahi-Sichani M, Davis RL. Novel, primate-specific PDE10A isoform highlights gene expression complexity in human striatum with implications on the molecular pathology of bipolar disorder. Transl Psychiatry. 2016 Feb;6(2):e742–e742.

28. Hu W, Lu T, Chen A, Huang Y, Hansen R, Chandler LJ, Zhang HT. Inhibition of phosphodiesterase-4 decreases ethanol intake in mice. Psychopharmacology. 2011 Nov 1;218(2):331–9.

29. Logrip ML, Vendruscolo LF, Schlosburg JE, Koob GF, Zorrilla EP. Phosphodiesterase 10A regulates alcohol and saccharin self-administration in rats. Neuropsychopharmacology. 2014 Jun;39(7):1722–31.

30. Logrip ML. Phosphodiesterase regulation of alcohol drinking in rodents. Alcohol. 2015 Dec 1;49(8):795–802.

31. de Laat B, Kling YE, Schroyen G, Ooms M, Hooker JM, Bormans G, Van Laere K, Ceccarini J. Effects of chronic voluntary alcohol consumption on PDE10A availability: a longitudinal behavioral and [18F]JNJ42259152 PET study in rats. Eur J Nucl Med Mol Imaging. 2022 Jan 1;49(2):492–502.

32. Wilson JM, Ogden AML, Loomis S, Gilmour G, Baucum AJ, Belecky-Adams TL, Merchant KM. Phosphodiesterase 10A inhibitor, MP-10 (PF-2545920), produces greater induction of c-Fos in dopamine D2 neurons than in D1 neurons in the neostriatum. Neuropharmacology. 2015 Dec 1;99:379–86.

33. Bertotto LB, Lampson-Stixrud D, Sinha A, Rohani NK, Myer I, Zorrilla EP. Effects of the Phosphodiesterase 10A Inhibitor MR1916 on Alcohol Self-Administration and Striatal Gene Expression in Post-Chronic Intermittent Ethanol-Exposed Rats. Cells. 2024 Jan;13(4):321.

34. Luísa B. Bertotto. Effects Of A PDE10A Inhibitor And Pde10a2 Deficiency On Voluntary Alcohol Intake In Mice. Poster Presentation presented at: Alcoholism and Stress: A Framework for Future Treatment Strategies; 2023 May 16.

35. Kovács KJ. Measurement of Immediate-Early Gene Activation- c-fos and Beyond. Journal of Neuroendocrinology. 2008;20(6):665–72.

36. Chan SHH, Chang KF, Ou CC, Chan JYH. Nitric Oxide Regulates c-fos Expression in Nucleus Tractus Solitarii Induced by Baroreceptor Activation via cGMP-Dependent Protein Kinase and cAMP Response Element-Binding Protein Phosphorylation. Mol Pharmacol. 2004 Feb 1;65(2):319–25.

37. Moens U, Subramaniam N, Johansen B, Aarbakke J. The c-*fos* cAMP-response element: Regulation of gene expression by a *β*2-adrenergic agonist, serum and DNA methylation. Biochimica et Biophysica Acta (BBA) - Gene Structure and Expression. 1993 Apr 29;1173(1):63–70.

38. Maronde E. Influence of Phosphodiesterase Inhibition on CRE- and EGR1-Dependent Transcription in a Mouse Hippocampal Cell Line. International Journal of Molecular Sciences. 2020 Jan;21(22):8658.

39. SILVERMAN ES, DU J, WILLIAMS AJ, WADGAONKAR R, DRAZEN JM, COLLINS T. cAMP-response-element-binding-protein-binding protein (CBP) and p300 are transcriptional co-activators of early growth response factor-1 (Egr-1). Biochemical Journal. 1998 Nov 15;336(1):183–9.

40. Ginty DD, Glowacka D, Bader DS, Hidaka H, Wagner JA. Induction of immediate early genes by Ca2+ influx requires cAMP-dependent protein kinase in PC12 cells. Journal of Biological Chemistry. 1991 Sep 15;266(26):17454–8.

41. Benito E, Valor LM, Jimenez-Minchan M, Huber W, Barco A. cAMP Response Element-Binding Protein Is a Primary Hub of Activity-Driven Neuronal Gene Expression. J Neurosci. 2011 Dec 14;31(50):18237–50.

42. Gentzel RC, Toolan D, Roberts R, Koser AJ, Kandebo M, Hershey J, Renger JJ, Uslaner J, Smith SM. The PDE10A inhibitor MP-10 and haloperidol produce distinct gene expression profiles in the striatum and influence cataleptic behavior in rodents. Neuropharmacology. 2015 Dec 1;99:256–63.

43. Nakatani A, Nakamura S, Kimura H. The phosphodiesterase 10A selective inhibitor, TAK-063, induces c-Fos expression in both direct and indirect pathway medium spiny neurons and sub-regions of the medial prefrontal cortex in rats. Neuroscience Research. 2017 Dec 1;125:29–36.

44. Suzuki K, Harada A, Suzuki H, Miyamoto M, Kimura H. TAK-063, a PDE10A Inhibitor with Balanced Activation of Direct and Indirect Pathways, Provides Potent Antipsychotic-Like Effects in Multiple Paradigms. Neuropsychopharmacol. 2016 Aug;41(9):2252–62.

45. Logrip ML, Gainey SC. Sex differences in the long-term effects of past stress on alcohol self-administration, glucocorticoid sensitivity and phosphodiesterase 10A expression. Neuropharmacology. 2020 Mar 1;164:107857.

46. Hsu YT, Liao G, Bi X, Oka T, Tamura S, Baudry M. The PDE10A inhibitor, papaverine, differentially activates ERK in male and female rat striatal slices. Neuropharmacology. 2011 Dec 1;61(8):1275–81.

47. Freeman-Cook KD, Hoffman RL, Johnson TW. Lipophilic efficiency: the most important efficiency metric in medicinal chemistry. Future Med Chem. 2013 Feb;5(2):113–5.

48. Shiao HY, Coumar MS, Chang CW, Ke YY, Chi YH, Chu CY, Sun HY, Chen CH, Lin WH, Fung KS, Kuo PC, Huang CT, Chang KY, Lu CT, Hsu JTA, Chen CT, Jiaang WT, Chao YS, Hsieh HP. Optimization of Ligand and Lipophilic Efficiency To Identify an in Vivo Active Furano-Pyrimidine Aurora Kinase Inhibitor. J Med Chem. 2013 Jul 11;56(13):5247–60.

49. Tarcsay Á, Nyíri K, Keserű GM. Impact of Lipophilic Efficiency on Compound Quality. J Med Chem. 2012 Feb 9;55(3):1252–60.

50. Johnson TW, Gallego RA, Edwards MP. Lipophilic Efficiency as an Important Metric in Drug Design. J Med Chem. 2018 Aug 9;61(15):6401–20.

51. Luísa B. Bertotto, Eleanna Sakoulas, Saumya Ranjan, Anush G. Ghoogasian, Solimar Rosado Iglesias, Sebastian Oakes, Giovana Macedo, Katrina Lin, Olivia Alcoran, Anastasia E. Pimentel, Eric P. Zorrilla. Effects of the phosphodiesterase 10A inhibitor AMG579 on striatal gene expression and ethanol self-administration in naïve and post-chronic intermittent ethanol exposed rats. 2023. Unpublished manuscript.

52. Cao J, Willett JA, Dorris DM, Meitzen J. Sex Differences in Medium Spiny Neuron Excitability and Glutamatergic Synaptic Input: Heterogeneity Across Striatal Regions and Evidence for Estradiol-Dependent Sexual Differentiation. Front Endocrinol (Lausanne). 2018 Apr 18;9:173.

53. Bonate R, Kurek G, Hrabak M, Patterson S, Padovan-Neto F, West AR, Steiner H. Phosphodiesterase 10A (PDE10A): Regulator of Dopamine Agonist-Induced Gene Expression in the Striatum. Cells. 2022 Jul 16;11(14):2214.

54. Fujishige K, Kotera J, Omori K. Striatum- and testis-specific phosphodiesterase PDE10A. European Journal of Biochemistry. 1999;266(3):1118–27.

55. Xie Z, Adamowicz WO, Eldred WD, Jakowski AB, Kleiman RJ, Morton DG, Stephenson DT, Strick CA, Williams RD, Menniti FS. Cellular and subcellular localization of PDE10A, a striatum-enriched phosphodiesterase. Neuroscience. 2006 Jan 1;139(2):597–607.

56. Dean RB, Dixon WJ. Simplified Statistics for Small Numbers of Observations. Anal Chem. 1951 Apr 15;23(4):636–8.

57. Rorabacher DB. Statistical treatment for rejection of deviant values: critical values of Dixon's "Q" parameter and related subrange ratios at the 95% confidence level. Anal Chem. 1991 Jan 15;63(2):139–46.

58. Weisberg S, Cook RD. Residuals and Influence in Regression. London & New York: Chapman & Hall; 1982.

59. van Ginkel JR, Linting M, Rippe RCA, van der Voort A. Rebutting Existing Misconceptions About Multiple Imputation as a Method for Handling Missing Data. Journal of Personality Assessment. 2020 May 3;102(3):297–308.

60. Suzuki K, Kimura H. TAK-063, a novel PDE10A inhibitor with balanced activation of direct and indirect pathways, provides a unique opportunity for the treatment of schizophrenia. CNS Neurosci Ther. 2018 Jul;24(7):604–14.

61. MacMullen CM, Fallahi M, Davis RL. Novel PDE10A transcript diversity in the human striatum: Insights into gene complexity, conservation and regulation. Gene. 2017 Mar 30;606:17–24.

62. Suzuki K, Harada A, Shiraishi E, Kimura H. In Vivo Pharmacological Characterization of TAK-063, a Potent and Selective Phosphodiesterase 10A Inhibitor with Antipsychotic-Like Activity in Rodents. J Pharmacol Exp Ther. 2015 Mar 1;352(3):471–9.

63. Heckman PRA, van Duinen MA, Bollen EPP, Nishi A, Wennogle LP, Blokland A, Prickaerts J. Phosphodiesterase Inhibition and Regulation of Dopaminergic Frontal and Striatal Functioning: Clinical Implications. Int J Neuropsychopharmacol. 2016 Apr 2;19(10):pyw030.

64. Corbit LH, Janak PH. Habitual alcohol seeking: Neural bases and possible relations to alcohol use disorders. Alcohol Clin Exp Res. 2016 Jul;40(7):1380–9.